

# Protein expression changes during human triple negative breast cancer cell line progression to lymph node metastasis in a xenografted model in nude mice

María Paula Roberti,<sup>1</sup> Juan Martín Arriaga,<sup>1</sup> Michele Bianchini,<sup>1</sup> Héctor Ramiro Quintá,<sup>2</sup> Alicia Inés Bravo,<sup>3</sup> Estrella Mariel Levy,<sup>1</sup> José Mordoh<sup>1,2</sup> and María Marcela Barrio<sup>1,\*</sup>

<sup>1</sup>Centro de Investigaciones Oncológicas; Fundación Cáncer and Instituto Alexander Fleming; Buenos Aires, Argentina; <sup>2</sup>Fundación Instituto Leloir; IIBBA-CONICET; Buenos Aires, Argentina; <sup>3</sup>Unidad de Inmunopatología; HIGA Eva Perón; San Martín, Argentina

**Keywords:** triple negative breast cancer, metastasis, protein profile, angiogenesis

Triple negative breast cancers (TNBC) lacking hormone receptors and HER-2 amplification are very aggressive tumors. Since relevant differences between primary tumors and metastases could arise during tumor progression as evidenced by phenotypic discordances reported for hormonal receptors or HER-2 expression, in this analysis we studied changes that occurred in our TNBC model IIB-BR-G throughout the development of IIB-BR-G<sub>-MTS6</sub> metastasis to the lymph nodes (LN) in nude mice, using an antibody-based protein array to characterize their expression profile. We also analyzed their growth kinetics, migration, invasiveness and cytoskeleton structure in vitro and in vivo.

In vitro IIB-BR-G<sub>-MTS6</sub> cells grew slower but showed higher anchorage independent growth. In vivo IIB-BR-G<sub>-MTS6</sub> tumors grew significantly faster and showed a 100% incidence of LN metastasis after s.c. inoculation, although no metastasis was observed for IIB-BR-G. CCL3, IL1 $\beta$ , CXCL1, CSF2, CSF3, IGFBP1, IL1 $\alpha$ , IL6, IL8, CCL20, PLAUR, PIGF and VEGF were strongly upregulated in IIB-BR-G<sub>-MTS6</sub> while CCL4, ICAM3, CXCL12, TNFRSF18, FIGF were the most downregulated proteins in the metastatic cell line. IIB-BR-G<sub>-MTS6</sub> protein expression profile could reflect a higher NF $\kappa$ B activation in these cells. In vitro, IIB-BR-G displayed higher migration but IIB-BR-G<sub>-MTS6</sub> had more elevated matrigel invasion ability. In agreement with that observation, IIB-BR-G<sub>-MTS6</sub> had an upregulated expression of MMP1, MMP9, MMP13, PLAUR and HGF. IIB-BR-G<sub>-MTS6</sub> tumors presented also higher local lymphatic invasion than IIB-BR-G but similar lymphatic vessel densities. VEGFC and VEGFA/B expression were higher both in vitro and in vivo for IIB-BR-G<sub>-MTS6</sub>. IIB-BR-G<sub>-MTS6</sub> expressed more vimentin than IIB-BR-G cells, which was mainly localized in the cellular extremities and both cell lines are E-cadherin negative.

Our results suggest that IIB-BR-G<sub>-MTS6</sub> cells have acquired a pronounced epithelial-to-mesenchymal transition phenotype. Protein expression changes observed between primary tumor-derived IIB-BR-G and metastatic IIB-BR-G<sub>-MTS6</sub> TNBC cells suggest potential targets involved in the control of metastasis.

## Introduction

Breast cancer (BC) is the most frequent tumor in women worldwide and although its mortality has significantly decreased in the past decades some tumors are still difficult to treat. Breast tumors can be categorized as luminal subtype A, luminal subtype B, HER-2<sup>+</sup>, basal subtype, normal breast-like, and the recently introduced claudin-low subtype, based on their molecular characteristics.<sup>1,2</sup> In the clinical routine BC is classified based on specific immunohistochemical markers that define different phenotypes. Triple negative breast cancers (TNBC), neither expressing estrogen receptor (ER), progesterone receptor (PR) nor HER-2, accounts for 10–20% of BC and are among the most aggressive tumors yet without effective therapies.<sup>3</sup> TNBC has common features overlapping with basal-like molecular class of

tumors and cancers carrying BRCA1 germ line mutation and in fact they are generally, but not constantly, of the basal subtype.<sup>4</sup> In addition, a subset of TNBC exists that also expresses vimentin. It is thought that this group represents BC that have undergone an epithelial-to-mesenchymal transition (EMT) and it has been associated to more invasive tumors, higher mitotic indexes and worse clinical outcome.<sup>5,6</sup>

Metastasis is a hallmark of most tumor types and the cause of the majority of cancer deaths. BC first disseminates via lymphatic vessels to their regional lymph nodes (LN); the axillary LN status is one of the most important prognostic variables in BC and a crucial component of the staging system. Several clinico-histopathological parameters are considered to be strong predictors of metastasis; however, they fail to accurately classify breast tumors according to their clinical behavior and to predict

\*Correspondence to: María Marcela Barrio; Email: mbarrio@conicet.gov.ar  
Submitted: 03/01/12; Revised: 06/13/12; Accepted: 06/20/12  
<http://dx.doi.org/10.4161/cbt.21187>

which patients will have disease recurrence. Although the connection between LN metastases, poor prognosis and shorter survival is clearly established, the active involvement of the lymphatic system in cancer metastasis remains still largely unknown. TNBC has a propensity for visceral metastasis to brain, and lung, rather than to LN, bone or liver.<sup>7</sup> This could be due to a trend of TNBC cells to disseminate through blood vessels rather than lymphatic spread. However, the presence of LN metastasis in TNBC patients is significantly associated to shorter overall survival (OS) and recurrence-free survival in comparison to node-negative patients, although the prognosis may not be affected by the number of positive LN.<sup>8</sup>

Protein expression, including predictive markers like hormone receptors and HER-2 can change during disease progression from primary to metastatic BC.<sup>9,10</sup> Several reports have shown that a discordant status for HER-2 and hormone receptors can be found when paired samples of primary and metastatic BC are compared and that these discordances could have an impact in treatment response in metastatic BC patients which is now only based in the primary tumor phenotype. Therefore, reassessment of these markers at the time of disease progression may help to optimize and personalize treatment decisions.<sup>11,12</sup> In this sense, many other proteins may also change during tumor progression, conferring metastatic cells different abilities to grow, invade distant places, drugs resistance and angiogenesis, that could have an impact in treatment decision and success.

Metastatic tissue can be difficult to obtain in the clinical setting because of the location of metastatic site to be compared with the paired primary tumor. To study protein expression changes taken place throughout the metastatic progression we thought to use human TNBC cell lines. The human cell line IIB-BR-G was originated from a primary breast tumor that did not express ER, PR or HER-2 and was tumorigenic in nude mice after subcutaneous (s.c.) inoculation.<sup>13</sup> A spontaneous metastatic variant (IIB-BR-G-MT) was obtained after 40 subcutaneous passages in nude mice. Metastases that grew in LN were excised and xenografted subcutaneously twice to enrich the tumor population with metastatic cells. IIB-BR-G<sub>MTS</sub> cells generated tumors that increased their growth rates in vivo, gave rise to LN in 100% of recipients, some mice also presenting lung micrometastases as we have previously shown.<sup>14</sup>

In the present work we performed a proteomic characterization of the LN-metastasis-derived IIB-BR-G<sub>MTS6</sub> TNBC cell line selected after six rounds of metastatic enrichment in nude mice. We compared this cell line to the parental non-metastatic IIB-BR-G cell line, using an antibody-based protein array that allows primarily the screening of chemokines, cytokines, growth factors and their receptors, in order to identify protein expression changes that could be associated to their metastatic phenotype.

## Results

**Description of IIB-BR-G and IIB-BR-G<sub>MTS6</sub> model.** After various s.c. inoculation in nude mice, IIB-BR-G cells developed spontaneous metastases in the axillary LNs which were excised, cultured in vitro for a few passages and re-inoculated in nude

mice s.c. After repeating this procedure for six times in order to enrich the population in metastatic cells, we generated IIB-BR-G<sub>MTS6</sub> cell line (Fig. 1A). In vitro, both IIB-BR- and IIB-BR-G<sub>MTS6</sub> cell lines grew as monolayers, although IIB-BR-G<sub>MTS6</sub> cells tended to be less adhesive with a heterogeneous morphology and did not reach confluence as IIB-BR-G cells did. Their growth curves were also different since IIB-BR-G cells grew faster with a doubling time of 55.96 h while the growth of IIB-BR-G<sub>MTS6</sub> cells was slower (doubling time 85.62 h) (Fig. 1B). However, anchorage-independent growth was significantly higher for IIB-BR-G<sub>MTS6</sub> cells as compared with IIB-BR-G as evidenced in soft agar clonogenic assays ( $p < 0.0001$ ) (Fig. 1C).

In vivo, IIB-BR-G<sub>MTS6</sub> s.c. tumors grew earlier and faster with a calculated doubling time of 6.8 d compared with IIB-BR-G tumors (doubling time 8.7 d) ( $p < 0.0001$ ) (Fig. 1D). Five weeks after inoculation IIB-BR-G<sub>MTS6</sub> s.c. tumors have large central necrotic areas probably due to hypoxia generated by fast growth. The same phenomenon was observed but only after 19 weeks for IIB-BR-G cells (not shown).

IIB-BR-G and IIB-BR-G<sub>MTS6</sub> cells inoculated s.c. in the back or in the mammary fat pad developed tumors in all recipients ( $n = 5$ ) and IIB-BR-G<sub>MTS6</sub> additionally developed metastases in axillary LN in 100% of mice by 5–6 weeks, while IIB-BR-G cells did not, even 19 weeks after inoculation (not shown). Metastases were evident macroscopically even in contralateral LN to the inoculated tumor. Metastasis to the LN was confirmed histologically after examination of hematoxylin-eosin stained sections (Fig. 1E–H). In some IIB-BR-G<sub>MTS6</sub> bearing mice some micrometastasis to the lungs could also be found (not shown).

**Proteomic analysis by antibody-based array comparing IIB-BR-G and IIB-BR-G<sub>MTS6</sub> cell lines showed an expression profile associated to metastasis.** An antibody array using 174 antibodies distributed in three glass slides allowed us to test the relative expression of 168 different proteins secreted into CM and present in cell extracts of IIB-BR-G and IIB-BR-G<sub>MTS6</sub> cell lines. This antibody array was selected to test the expression changes of cytokines, growth factors and chemokines that could be related to the metastatic ability of IIB-BR-G<sub>MTS6</sub> cells relative to that of IIB-BR-G. All significantly deregulated proteins in IIB-BR-G<sub>MTS6</sub> compared with IIB-BR-G cells are shown in Tables 1 and 2, corresponding to secreted proteins into CM and present in cell extracts, respectively. The relative expression values for all tested proteins that remained unchanged ( $\log_2$  relative expression IIB-BR-G<sub>MTS6</sub>/IIB-BR-G between 1 and -1) are shown in Table S1 and S2.

The analysis of CM showed that IIB-BR-G<sub>MTS6</sub> secretion was higher for 37 proteins and lower for 27 while the other proteins remained unchanged. The most upregulated IIB-BR-G<sub>MTS6</sub> secreted proteins (CM) were IL1 $\beta$ , IGFBP1, GRO $\alpha$ /CXCL1, MIP-3 $\alpha$ /CCL20, GM-CSF/CSF3, GCSF/CSF2, IL2R  $\alpha$ , IL1 $\alpha$ , IL6 and VEGFA. Among the less secreted proteins we found VEGFD, SDF1- $\beta$ /CXCL12, ICAM3, MMP13, AgRP, IL12 p40, FGF9, GITR-Ligand and MIP-1 $\beta$ /CCL4.

For some proteins signal in the antibody array was negative for both cells lines (less than two times negative controls signal), such as l-selectin (expressed in neutrophils), NGF

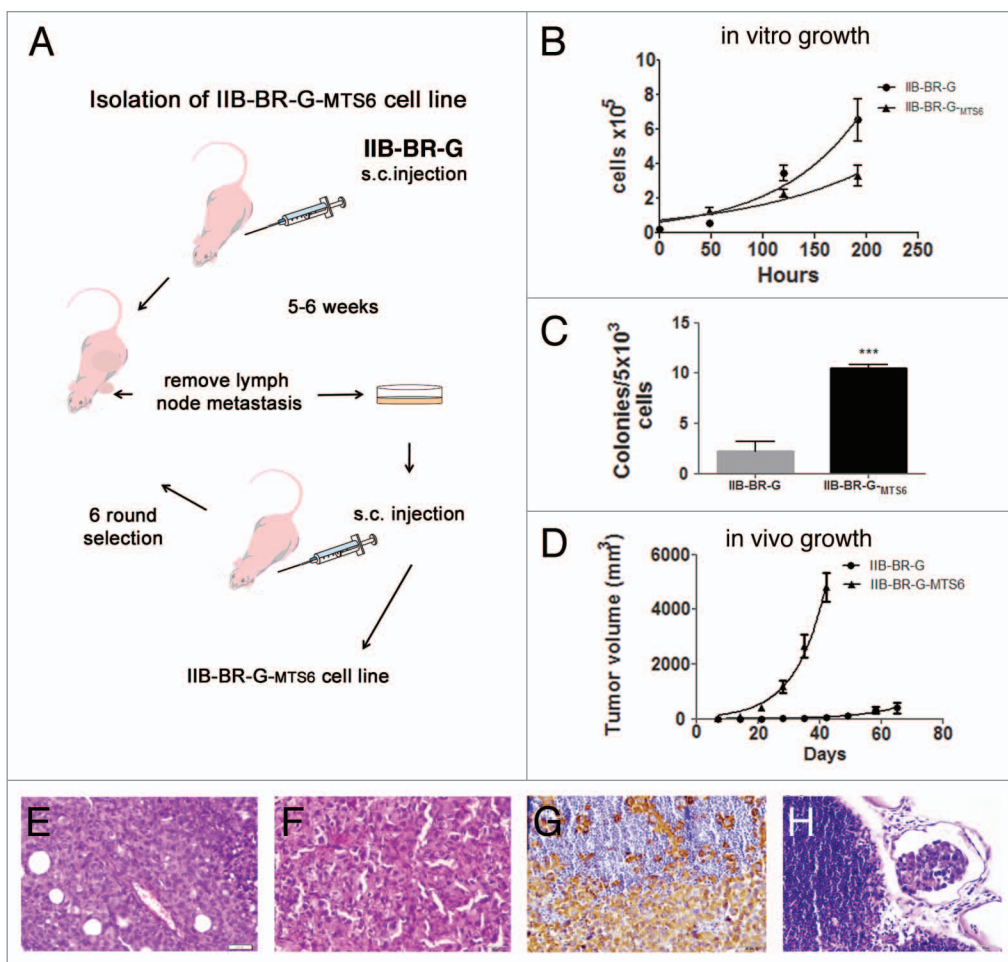


**Figure 1.** IIB-BR-G and IIB-BR-G<sub>MTS6</sub> TNBC cell lines. (A) IIB-BR-G<sub>MTS6</sub> cell line was obtained after six rounds of enrichment in metastatic cells to the LN, after initial s.c. injection of IIB-BR-G cells into nude mice. (B) In vitro tumor cell growth. IIB-BR-G and IIB-BR-G<sub>MTS6</sub> cell growth was assessed by the MTT method in quadruplicate. Results are shown as mean  $\pm$  SD. (C) Anchorage independent cell growth. Clonogenic assays for IIB-BR-G and IIB-BR-G<sub>MTS6</sub> were performed in triplicate. Data show the number of counted colonies as mean  $\pm$  SD. \*\*\*statistically highly significant,  $p < 0.0001$  (t-test). (D) In vivo growth curves. IIB-BR-G and IIB-BR-G<sub>MTS6</sub> were injected s.c. in nude mice ( $n = 5$ ) and tumor volumes were measured during 9 and 6 weeks, respectively. Result is shown as mean  $\pm$  SD. Histological analysis of xenografted tumors. IIB-BR-G (E) and IIB-BR-G<sub>MTS6</sub> (F) HE staining. (G) Vimentin immunohistochemistry in IIB-BR-G<sub>MTS6</sub> LN metastasis. (H) IIB-BR-G<sub>MTS6</sub> LN metastasis HE staining where an afferent lymph vessel containing a tumor emboli is shown. Scale bar = 20  $\mu\text{m}$ .

(nerve growth factor), IL-2R $\gamma$ , IP-10/CXCL10, secreted by monocytes and lymphocytes, TECK/CCL25, (expressed in small intestine and thymus) and CK  $\beta$  8–1. Also, in CM of both cell lines some receptors like EGFR, IL2RA, were detected presumably shed into the CM or derived from dead cells.

With respect to cell extracts, IIB-BR-G<sub>MTS6</sub> showed upregulation of 24 proteins and downregulation of 6 compared with parental IIB-BR-G. The most upregulated proteins were MIP-1  $\alpha$ /CCL3, GCSF/CSF3, IL2Ra, CXCL1, PlGF and Adiponectin (APM1). Downregulation in IIB-BR-G<sub>MTS6</sub> was found for Siglec5, TNFRSF21, IL2Rb and VEGFR2 (KDR). No expression of NGF, IL1 R4/ST2, IL1R1, IL1R2, IL11, L-Selectin, IP-10 or IL2 R $\gamma$ , was observed for both cell lines.

We used EASE annotation tool to disclose the potential biological relevance of the differentially expressed proteins that could be related to the metastatic phenotype we used. Using Gene Ontology Annotation we identified some functional

categories that were over-represented among the IIB-BR-G<sub>MTS6</sub> deregulated proteins recognized in the antibody array. Table 3 shows the combined CM and cell extracts results of the EASE analysis. It also revealed that expression of proteins located in chromosome 7 is significantly altered in IIB-BR-G<sub>MTS6</sub> cells ( $p = 0.0069$ ) since six of them located in 7p (EGFR, IGFBP1, IGFBP3, IL6, INHBA, PDGFA) and one in 7q (HGF) have increased their expression in IIB-BR-G<sub>MTS6</sub> as compared with IIB-BR-G cells.

To further investigate the biological relevance of genes that were up or downregulated in metastatic IIB-BR-G<sub>MTS6</sub> relative to primary tumor-derived IIB-BR-G we queried PubMed manually. Based on the potential function of BC cancer cells and their relationship with metastasis, we collected those deregulated proteins in IIB-BR-G<sub>MTS6</sub> cells that could be potentially associated to the metastatic ability and explored the previously published evidences. Grouped by their known role some of these

**Table 1.** Deregulated secreted proteins in IIB-BR-G<sup>-MT56</sup> CM compared with parental IIB-BR-G

Name in antibody array	Gene symbol	Description	Log <sub>2</sub> fold change
<b>Chemokines, cytokines and their receptors</b>			
IL-1 β	IL1b	Interleukin 1, β	8.17
GRO-α	CXCL1	Chemokine (CXC motif) ligand 1	6.87
MIP-3 α	CCL20	Chemokine (c-c motif) ligand 20	6.71
IL-2 R α	IL2RA	Interleukin 2 receptor, α	5.55
IL-1 α	IL1a	Interleukin 1, α	5.44
IL-6	IL6	Interleukin 6	4.65
IL-4	IL4	Interleukin 4	4.26
MCP-2	CCL8	Chemokine (c-c motif) ligand 8	3.19
IL-8	IL8	Interleukin 8	2.63
CXCL-16	CXCL16	Chemokine (CXC-motif) ligand 16	2.59
GCP-2	CXCL5	Chemokine (CXC-motif) ligand 5	2.42
RANTES	CCL5	Chemokine (C-C-motif) ligand 5	1.66
NAP-2/CXCL7	CXCL7	Chemokine (CXC-motif) ligand 7	1.64
PARC	CCL18	Chemokine (CC-motif) ligand 18	1.36
IL-18 BP α	IL18	Interleukin 18	1.33
sgp130	IL6st	Interleukin 6 signal transducer (gp130, oncostatin receptor)	1.18
TARC	CCL17	Chemokine (CC-motif) ligand 17	1.15
IL-18Rbeta	IL18RB	Interleukin 18 receptor β	-1.02
I-TAC	CXCL11	Chemokine (CXC-motif) ligand 11	-1.18
HCC-4	CCL16	Chemokine (CC motif) ligand 16	-1.31
IL-11	IL11	Interleukin 11	-1.43
IL-1RI	IL1RI	Interleukin 1 receptor, type I	-1.49
MIG	CXCL9	Chemokine CXC-motif	-1.73
IL-12 p70	IL12	Interleukin 12	-1.87
IFN gamma	IFNG	Interferon, gamma	-2.1
MIP-3 β	CCL19	Chemokine (CC-motif) ligand 19	-2.43
MIP-1 β	CCL4	Chemokine (CC-motif) ligand 4	-4.49
SDF-1 β	CXCL12	Chemokine (CXC-motif) ligand 12	-4.82
<b>Growth and differentiation factors, receptors and regulators</b>			
IGFBP-1	IGFBP1	Insulin growth factor binding protein 1	8.17
GM-CSF	CSF2	Granulocyte-macrophage colony stimulating factor	6.01
G-CSF	CSF3	Granulocyte colony stimulating factor	5.92
sTNF-RI	TNFRSF1A	Tumor necrosis factor receptor superfamily, member 1 A	3.65
PDGFAA	PDGFA	Platelet derived growth factor A	3.23
IGFBP-6	IGFBP6	Insulin growth factor binding protein 6	3.18
EGF-R	EGFR	Epidermal growth factor receptor	3.11
LAP	TGFB1	Tumor growth factor β 1	2.84
IGFBP-4	IGFBP4	Insulin growth factor binding protein 4	2.30
NT-4	NTF5	Neurotrophic growth factor 4	1.50
IGFBP-3	IGFBP3	Insulin growth factor binding protein 3	1.41
Osteoprotegerin	TNFRSF11B	Tumor necrosis factor receptor superfamily, member 11B	1.11
TRAIL R3	TNFRSF10C	Tumor necrosis factor receptor superfamily, member 10C	-1.14
Oncostatin M	OSM	Oncostatin M	-1.19

Log<sub>2</sub> fold change: log<sub>2</sub> of positive control normalization without background sample IIB-BR-G<sup>-MT56</sup>/positive control normalization without background sample IIB-BR-G.

**Table 1.** Deregulated secreted proteins in IIB-BR-G<sub>-MTS6</sub> CM compared with parental IIB-BR-G (continued)

Growth and differentiation factors, receptors and regulators			
HGF	HGF	Hepatocyte growth factor	-1.20
BTC	BTC	Betacellulin	-1.75
FGF-9	FGF9	Fibroblast growth factor 9 (glia-activating factor)	-3.86
GITR-ligand	TNFRSF18	Tumor necrosis factor receptor superfamily, member 18	-4.23
Cell adhesion, angiogenesis and invasion related			
VEGF	VEGF	Vascular endothelial growth factor	4.62
Angiogenin	Ang	Angiogenin, ribonuclease, RNase A family, 5	4.56
ICAM-1	ICAM1	Intercellular adhesion molecule 1	4.3
BMP-7	BMP7	Bone morphogenetic protein 7	4.21
uPAR	PLAUR	Urokinase-type Plasminogen activator receptor	4.17
bFGF	FGF2	Basic fibroblast growth factor	1.81
<b>TIMP1</b>	<b>TIMP1</b>	<b>metallopeptidase inhibitor 1</b>	<b>1.65</b>
Activin A	INHBA	Inhibin A	1.38
Tie-2	TEK	TEK tyrosine kinase endotelial	-1.35
MMP-13	MMP13	matrix metalloproteinase 13 (collagenase 3)	-3.06
ICAM-3	ICAM-3	Intercellular adhesion molecule 3	-4.54
VEGF-D	FIGF	Vascular endotelial factor D	-5.83
Others			
Siglec-5	Siglec5	Sialic acid binding Ig-like lectin 5	-1.19
CD14	CD14	Monocyte differentiation antigen CD14	-1.36
Prolactin	Prl	prolactin	-2.22
Agrp	AGRP	Agouti related protein homolog	-3.4

Log<sub>2</sub> fold change: log<sub>2</sub> of positive control normalization without background sample IIB-BR-G<sub>-MTS6</sub>/positive control normalization without background sample IIB-BR-G.

proteins briefly presented below along with results of additional experiments.

**Proliferation and survival related proteins.** The oncogenic pathway EGFR-RAS signaling could have contributed to the autonomous cell proliferation in both cell lines as we have previously shown.<sup>15</sup> Through the antibody array assay several growth factors were found upregulated in the IIB-BR-G<sub>-MTS6</sub> cells like CSF3, PIGF, CSF2, PDGF AA, PDGF AB, FGF2/bFGF, and the regulatory IGFBP1, 6, 4 and 3, as compared with non-metastatic IIB-BR-G. Some of these molecules could have a direct autocrine growth promoting effect but also could influence tumor stromal cells contributing to tumor growth. Also, IIB-BR-G<sub>-MTS6</sub> cell secrete significantly more IL4 to CM (4.26 log<sub>2</sub> fold change) than IIB-BR-G. Of note, despite its immune modulating activity IL4 has been shown to act as an autocrine survival factor in epithelial cancers.<sup>16</sup> Thus, production of some growth factors in metastatic IIB-BR-G<sub>-MTS6</sub> cells could be a relevant change in protein expression relative to IIB-BR-G cells, facilitating cells growth that could serve to explain faster in vivo growth of IIB-BR-G<sub>-MTS6</sub> s.c. xenografts as compared with IIB-BR-G.

**Angiogenesis and lymphangiogenesis related proteins.** One critical event for tumor growth and metastasis is the generation of a new network of blood vessels that can be promoted by several cytokines produced by tumor or stroma cells. Several pro-angiogenic factors are upregulated in IIB-BR-G<sub>-MTS6</sub> cells and /or

secreted into their CM compared with non-metastatic IIB-BR-G cell line: CXCL1, IL8, IL1 $\beta$ , IL1 $\alpha$ , VEGFA, angiogenin/ANG, HGF, PIGF, LAP-TGF $\beta$ 1 (latent TGF $\beta$ 1), FGF2/bFGF and TEK (tie2, angiopoietin receptor) (Tables 1 and 2). In vitro IIB-BR-G<sub>-MTS6</sub> cells secreted much more vascular endothelial growth factor (VEGFA) to the CM but less VEGFD/FIGF. Both cell lines showed similar VEGFR3/FLT4 expression in cell extracts (Table S2) but VEGFR2/KDR, was downregulated in IIB-BR-G<sub>-MTS6</sub> cells (Table 2).

Since VEGFA is strongly upregulated in IIB-BR-G<sub>-MTS6</sub> cells in vitro, and its expression has been associated to higher LVD,<sup>17</sup> we evaluated its expression in vivo by immunostaining of nude mice s.c. xenografts. As shown in Figure 2 both IIB-BR-G and IIB-BR-G<sub>-MTS6</sub> tumors showed blood vessels and microvessels stained with an anti-VEGFA/B mAb and also tumor cells showed membrane staining. Some of the VEGFA/B expressing cells seemed incipient structures that could reflect neoangiogenesis or vasculogenic mimicry. The positive staining area in IIB-BR-G<sub>-MTS6</sub> tumors was 2.99 times higher than in IIB-BR-G tumors ( $p = 0.044$ , t-test), evidencing higher VEGFA/B in vivo expression associated to the metastatic cells (not shown). Also, CD31 staining allowed us to evaluate the presence of blood vessels, microvessels and some positive cells without a definite structure distributed through the tumor (Fig. 2). CD31 positive areas were thus quantified instead of blood vessel counts to better

**Table 2.** Deregulated proteins in IIB-BR-G<sub>-MTS6</sub> cell extracts secreted compared with parental IIB-BR-G

Name in antibody array	Gene symbol	Description	Log <sub>2</sub> fold change
<b>Chemokines, cytokines and their receptors</b>			
MIP-1 $\alpha$	CCL3	chemokine (c-c motif) ligand 3	8.9
IL-2 Ralpha	IL2Ra	Interleukin2receptor, $\alpha$	6.5
GRO- $\alpha$	CXCL1	chemokine (c-x-c motif) ligand 1	6.1
Acrp30	Adipoq (APM1)	Adiponectin	3.5
IL-8	IL8	interleukin 8	2.4
ActivinA	INHBA	Inhibin, $\beta$ A (activin A, activin AB $\alpha$ polypeptide)	2.4
sgp130I	IL6st	Interleukin 6 signal transducer (gp130, oncostatin M receptor)	1.8
IL6-R	IL6R	Interleukin 6 receptor	1.7
MPIF-1	CCL23	Chemokine (C-C motif) ligand 23	1.7
IL-12p70	IL12	Interleukin 12	1.2
ENA-78	CXCL5	Chemokine(C-X-C motif) ligand 5	1.1
IL-2 Rbeta	IL2RB	Interleukin 2 receptor, $\beta$	-2.1
<b>Growth and differentiation factors, receptors and regulators</b>			
GCSF	CSF3	Colony stimulating factor 3 (granulocyte)	8.7
PIGF	PIGF	Placental growth factor	4.6
TRAIL R4	TNFRSF10D	Tumor necrosis factor receptor superfamily, member 10d, decoy with truncated death domain	2.4
FGF-9	FGF9	Fibroblast growth factor 9 (glia-activating factor)	2
PDGF-AB	PDGF	Platelet derived growth factor polypeptide	1.6
HGF	HGF	Hepatocyte growth factor (hepatopoietin A, scatter factor)	1.2
Tie-1	TIE	Tyrosine kinase with immunoglobulin and epidermal growth factor homology domain	-1.2
DR6	TNFRSF21	Tumor necrosis factor receptor superfamily, member 21	-3.4
uPAR	PLAUR	Platelet/endothelial adhesion molecule 1	2.8
Tie-2	TEK	TEK tyrosine kinase endothelial	2.1
ICAM-3	ICAM3	Intercellular adhesion molecule 3	2
MMP-1	MMP1	matrix metalloproteinase 1 (interstitial collagenase)	2
MMP-13	MMP13	matrix metalloproteinase 13 (collagenase 3)	1.8
MMP-9	MMP9	Matrix metalloproteinase 9 (galatinase B, 92kDa gelatinase, 92kDa type IV collagenase)	1.2
ICAM-1	ICAM1	Intercellular adhesion molecule 1	1.2
PECAM-1	PECAM1	platelet/endothelial cell adhesion molecule 1	1.2
VEGFR2	KDR	kinase insert domain protein receptor	-1.9
<b>Others</b>			
SIGLEC-5	SIGLEC5	Sialic acid binding Ig-like lectin 5	-3.2

Log<sub>2</sub> fold change: log<sub>2</sub> of positive control normalization without background sample IIB-BR-G<sub>-MTS6</sub>/positive control normalization without background sample IIB-BR-G.

reflect angiogenesis. In this case, CD31 positive areas were 1.89 times higher in IIB-BR-G<sub>-MTS6</sub> tumors compared with IIB-BR-G though in the limit of significance ( $p = 0.051$ ,  $t$ -test).

It has been demonstrated that activation of lymphatic endothelium by VEGFC is crucial for tumor cell entry and migration via lymphatic vessels. Anti-VEGFC mAb was not included in the selected antibody-array that we used, thus we measured its expression by qRT-PCR in IIB-BR-G and IIB-BR-G<sub>-MTS6</sub> cell lines as well as in nude mice xenografts. As observed in **Figure 3A**

both cell lines express VEGFC, however, higher expression in metastatic IIB-BR-G<sub>-MTS6</sub> tumors was found as compared with IIB-BR-G *in vivo*. As mentioned above, VEGFR3, the specific receptor for VEGFC was equally expressed by IIB-BR-G<sub>-MTS6</sub> and IIB-BR-G cells.

Next, we evaluated the lymphatic vessel density (LVD) in IIB-BR-G<sub>-MTS6</sub> and IIB-BR-G *s.c.* xenografts by immunostaining with anti-podoplanin, a specific marker of lymphatic endothelium. As observed in **Figure 3B**, no significant differences

**Table 3.** Functional categories represented among deregulated proteins in IIB-BR-G<sub>-MTS6</sub> vs IIB-BR-G

Annotation tool	Functional category	EASE* Score	Protein
GO Biological Process	response to wounding	9.07e-003	↑IL1α; IL1β; IL4; IL8, CCL17; CCL18; CCL20; CCL23; CXCL5; CCL3; CCL5; CCL8; CSF2; CSF3; CXCL1; ↓CCL16; CXCL11; CXCL12 CCL19; CXCL9; CCL4;
GO Biological Process	cell growth and/or maintenance	7.82e-003	↑CCL23; CCL3; CCL5; PDGFA; LAP-TGFβ1 TIMP1; CCL8; CSF3; CXCL1; CXCL5; EGFR; FGF2; FGF9; HGF; IGFBP1; IGFBP3; IGFBP4; IGFBP6; IL1α; IL1β; IL4; IL6; IL6R; IL8; ↓OSM; BTC; CCL19 CCL4; CXCL12 FIGF; IFNγ
GO Biological Process	chemotaxis	2.37e-003	↑CCL17; CCL18; CCL20; CCL23; CCL3; CCL5; CCL8; CXCL1; CXCL12; CXCL5; CXCL9; FGF2; IL1α; IL4; IL8 ↓CCL16; CCL4; CCL19; CXCL11
Organismal role	cell migration/motility	2.36e-003	↑CCL17; CCL18; CCL20; CCL23; CCL3; CCL5; CCL8; CXCL1; CXCL12; CXCL5; CXCL9; FGF2; HGF; IFNγ; IGFBP3; IL4; IL8; PECAM1 ↓CCL16; CCL19; CCL4 CXCL11
GO Biological Process	response to stress	4.11e-002	↑CCL17; CCL20; CCL23; CCL3; CCL5; CCL8; CSF2; CSF3; CXCL1; CXCL11; CXCL12; CXCL5; CXCL9; IL1α; IL1β; IL4; IL6; IL8 ↓CCL16; CCL18, CCL19, CCL4
GO Molecular Function	glycosaminoglycan binding/heparin binding	2.92e-002	↑CCL23; CCL3; FGF9
GO Molecular Function	hydrolase activity/macromolecule catabolism	1.77e-002	↑ANG; HGF; MMP1; MMP13; MMP9; TIMP1
GO Biological Process	regulation of cell proliferation	1.56e-002	↑CCL23; CCL3; CSF3; CXCL1; CXCL5; FGF2; TGFβ1-LAP; TIMP1; IGFBP6; IL1α; IL1β; IL6; IL8; ↓OSM; BTC; FIGF
GO Biological Process	inflammatory response/ innate immune response	1.47e-002	↑IL1α; IL1β; IL8; CCL17; CCL18; CCL20; CCL23; CCL3; CCL5; CCL8; CXCL1; CXCL11; CXCL5; ↓CXCL12; CCL4CXCL9; CCL16; CCL19;
GO Biological Process	cell-cell signaling	1.29e-002	↑CCL17; CCL20; CCL23; CCL3; CCL5; CCL8; CSF3; CXCL5; FGF2; IL1α; LAP-TGFβ1; IL1β; IL6; IL8; PDGFA ↓CCL16; CCL4; FGF9; IFNγ; CXCL11; CXCL9; CCL18; CXCL12; TEK

Functional categories were obtained using EASE software as described in Methods. Results correspond to total deregulated IIB-BR-G<sub>-MTS6</sub> proteins (upregulated and downregulated) combining cell extracts plus CM results. EASE scores < 0.05 were considered significant. ↑ = protein upregulated in IIB-BR-G<sub>-MTS6</sub> vs. IIB-BR-G; ↓ = protein downregulated in IIB-BR-G<sub>-MTS6</sub> vs. IIB-BR-G.

in LVD were found between IIB-BR-G<sub>-MTS6</sub> and IIB-BR-G tumors. In **Figure 3C** examples of podoplanin immunostaining for both s.c. tumors are shown. In IIB-BR-G<sub>-MTS6</sub>, evaluation of LN metastasis with anti-podoplanin revealed many tumor cells located adjacent to lymphatic vessels and also emboli in the lumen of afferent lymph vessels evidencing lymphatic invasion (**Fig. 1H**). Our results suggest that increase of pro-angiogenic and lymphangiogenic factors expression has occurred in IIB-BR-G<sub>-MTS6</sub> cells after metastatic progression probably enabling tumor cells to generate more vascularized tumors and help facilitate tumor lymphatic invasion.

**IIB-BR-G<sub>-MTS6</sub> cells expression profile could be related to their higher in vitro invasiveness.** IIB-BR-G<sub>-MTS6</sub> cells exhibit higher expression of latency-associated peptide (LAP-TGFβ1) than IIB-BR-G, while other members of the TGFβ superfamily tested in the array, such as TGFβ1, TGFβ2, TGFβ3 and endoglin remained unchanged (**Table 1** and **Tables S1** and **S2**).

TGFβ1 is synthesized as a large precursor molecule consisting of an N-terminal prodomain (LAP) and a C-terminal mature domain. LAP acts as a multifunctional peptide that extracellularly confers latency to TGFβ1.<sup>18</sup> TGFβ has opposite roles in BC cancer progression either acting as a tumor suppressor in the initial phase, or stimulating invasion and metastasis at later stages. It is known that TGFβ-induced invasion is related to metalloproteinases MMP2 and MMP9 expression.<sup>19</sup> Cell-associated MMP9 is upregulated in IIB-BR-G<sub>-MTS6</sub> cells as compared with IIB-BR-G (log<sub>2</sub> fold change 1.2, **Table 2**). We also validated MMP9 expression by zymogram using gelatin as a substrate and found that IIB-BR-G<sub>-MTS6</sub> expressed more active MMP9 than IIB-BR-G cells (**Fig. 4A**).

In an in vitro assay we tested both cellular migrations through 8 μm pore filters and invasiveness using matrigel-coated filters. Although IIB-BR-G cells migrated more toward FBS (chemoattractant), IIB-BR-G<sub>-MTS6</sub> cells showed higher matrigel invasion

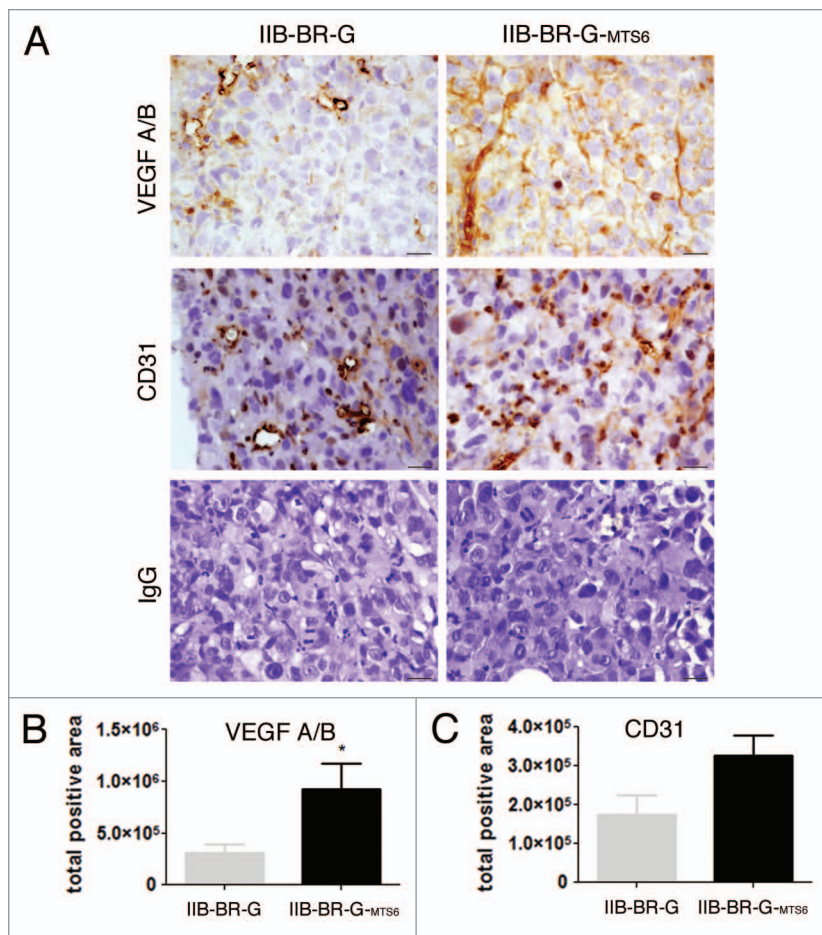


**Figure 2.** Angiogenesis related analyses. (A) VEGFA/B and CD31 stains were performed in IIB-BR-G and IIB-BR-G<sub>MTS6</sub> nude mice xenografts. An example of each immunostaining is shown for IIB-BR-G and IIB-BR-G<sub>MTS6</sub> xenografts. Also, an irrelevant mouse IgG was used as a negative control. Scale bar = 10 $\mu$ m. (B) VEGF A/B and CD31 positive stained areas were calculated for two different xenografts from each cell line as detailed in Methods. Results are indicated as mean  $\pm$  SD positive area. \*Statistically significant  $p < 0.05$  (t-test).

( $p < 0.05$ ) (Fig. 4B and C). IIB-BR-G<sub>MTS6</sub> cells showed more invasive ability in vitro which could be related to their higher expression of MMP9, MMP1, MMP13 and HGF that could facilitate matrigel degradation. Other upregulated molecule in IIB-BR-G<sub>MTS6</sub> cells is PLAUR (urokinase type plasminogen activator receptor) (2.8 log<sub>2</sub> fold change) compared with IIB-BR-G. PLAUR is a key molecule for pericellular proteolysis in tumor cell invasion and metastasis.<sup>20</sup>

**IIB-BR-G<sub>MTS6</sub> cell line expression profile suggests higher level of NF $\kappa$ B activation relative to parental IIB-BR-G cells.** Several of the IIB-BR-G<sub>MTS6</sub> upregulated proteins correspond to gene products that are possible inducers of NF $\kappa$ B like GM-CSF, HGF, IL1 and also gene products regulated by NF $\kappa$ B like VEGF, IL6, IL8, MMP9 and MMP13. As a whole, this expression profile suggests a higher NF $\kappa$ B level of activation in IIB-BR-G<sub>MTS6</sub> than in IIB-BR-G, which could be related to their metastatic ability. NF- $\kappa$ B is a crucial factor that is implicated in oncogenic pathways and also regulates immunoinflammatory responses. High level of activation of NF $\kappa$ B has been reported in specific

subtypes of BC, particularly those tumors that express erbB2 and are ER negative<sup>21</sup> but tumors expressing EGFR (ErbB1) may also be equally dependent of competent NF $\kappa$ B.<sup>22</sup>

**Cytokines, chemokines and metastasis.** In IIB-BR-G<sub>MTS6</sub> metastatic cells combining cell-associated and secretion to CM results, the more upregulated cytokines/chemokines were IL1 $\beta$ , CXCL1, CCL3, CCL20, IL1 $\alpha$ , IL6, CXCL8/IL8, IL4, CCL8, CXCL16, and the less expressed were CXCL12, CCL4, CCL19 compared with the parental IIB-BR-G cell line (Tables 1 and 2). Chavey et al. reported that multiple cytokines were overexpressed in ER negative BC and correlated with the inflammatory cell content and aggressiveness of the tumors.<sup>23</sup> IL1 $\beta$  is the most over-secreted cytokine in IIB-BR-G<sub>MTS6</sub> CM vs. IIB-BR-G and also IL1 $\alpha$  is overexpressed. Of note, numerous in vitro and in vivo models have linked IL1 $\beta$  production to tumor cell migration, MMP9 and ICAM1 expression (both upregulated in IIB-BR-G<sub>MTS6</sub> cells compared with IIB-BR-G), angiogenesis and activation of NF $\kappa$ B signaling pathway.<sup>24</sup> Interestingly, IIB-BR-G<sub>MTS6</sub> cells CXCL12 (SDF-1) secretion is downregulated compared with IIB-BR-G non-metastatic cells. CXCL12 production has been associated to metastasis limitation by inhibiting CXCR4 signaling in melanoma, breast and colon cancer.<sup>25</sup>

**EMT features in TNBC cell lines IIB-BR-G and IIB-BR-G<sub>MTS6</sub>.** Of note, the basal like BC subtype-associated marker CX3CL1/fractalkine is among the unchanged molecules expressed by both TNBC IIB-BR-G and IIB-BR-G<sub>MTS6</sub> cells. Also, we have previously shown that high vimentin expression is found in both cell lines by immunocytochemistry.<sup>15</sup> IIB-BR-G<sub>MTS6</sub> cells express much more PIGF than IIB-BR-G cells (Table 2), a known vimentin stabilizer.<sup>26</sup> In light of these results we confirmed that both cell lines expressed intermediate filament vimentin as detected by western blot (Fig. 5A), but IIB-BR-G<sub>MTS6</sub> presented higher expression. This higher vimentin expression in IIB-BR-G<sub>MTS6</sub> cells was also confirmed by confocal microscopy ( $p < 0.05$ ) (Fig. 5B) which also showed that both cell lines present highly organized actin F structures and that vimentin is mainly localized at cell extremes in IIB-BR-G<sub>MTS6</sub> cells which displayed a spindle-like morphology (Fig. 5C). Moreover, with a 3D-topographical analysis and a plot-profile it was demonstrated that only IIB-BR-G<sub>MTS6</sub> cells present vimentin surrounded by microfilaments at these extremes. This observation could be due to the reorganization of actin cytoskeleton as the cell becomes motile, and which has been reported for other cancer cells.<sup>27</sup> E-cadherin was not expressed in both cell lines as determined by immunocytochemistry (Fig. S3). Altogether these results suggest that IIB-BR-G<sub>MTS6</sub> cells have undergone a pronounced epithelial-to-mesenchymal-transition (EMT) probably associated to their metastatic behavior.

## Discussion

Although a great number of molecules have been associated to BC metastasis the mechanisms used by tumor cells to achieve the metastatic cascade are still poorly understood. Over the last years a bulk of evidence suggests the existence of a complex interaction between tumor cells and the blood and lymphatic endothelium in which an important role of chemokines and cytokines is emerging,<sup>28</sup> sharing many similarities with leukocyte trafficking. Acting either in a paracrine manner to modulate the activity of surrounding cells or in an autocrine fashion, cytokines perform a wide variety of functions. Aberrant expression of cytokines has been implicated in tumor cell growth, survival, migration, invasion, angiogenesis and modulation of the immune system interaction with the tumor.<sup>29,30</sup>

The use of spontaneously metastatic human BC cell lines provides a promising model to investigate the metastatic process. Because of the complexity and heterogeneity of BC no single model would be expected to mimic all aspects of the disease. Thus, it is necessary to develop models to evaluate treatments for metastatic disease and to enhance our understanding of the mechanisms that underlie metastatic progression.<sup>31</sup> LN metastasis was modeled in nude mice by IIB-BR-G<sub>MTS6</sub> cells s.c. inoculation resulting in the spontaneous formation of LN tumors. Our findings showed incremented expression of multiple growth factors, pro-angiogenic/lymphangiogenic factors, metalloproteinases, chemokines and pro-inflammatory cytokines potentially relevant to the metastatic steps such as autocrine growth control, migration, interaction with stromal cells, angiogenesis, lymphangiogenesis and invasion. Despite TNBC has a propensity for visceral metastasis to brain, and lung, rather than LN, bone or liver,<sup>7</sup> since IIB-BR-G<sub>MTS6</sub> cells growing in nude mice were selected based on the generation of LN metastasis, their changes in protein expression relative to parental IIB-BR-G cells might be more related to this latter process. The scheme in Figure 6 represents a proposed model that integrates IIB-BR-G<sub>MTS6</sub> protein expression profile with the different steps of the metastatic cascade.

We did not observe a discordant phenotype between IIB-BR-G and IIB-BR-G<sub>MTS6</sub> cells regarding hormonal status, HER-2 overexpression since both are TNBC as we have previously shown.<sup>14</sup> Also both cell lines express EGFR and have a mutated K-RAS status which could contribute to their autonomous cell proliferation and also to the modulation of gene expression to generate a tumor-promoting microenvironment.<sup>14</sup> EGFR-RAS activation has been shown to lead to increased secretion of IL8 and CXCL1 by tumor cells.<sup>32</sup> These chemokines in turn enhance tumor growth via an autocrine loop and promote tumor-associated angiogenesis. Despite this fact, we observed significant changes in other protein expression in IIB-BR-G<sub>MTS6</sub> metastatic cells as compared with IIB-BR-G. EGFR, IL8 and CXCL1 are among the most upregulated proteins compared with the non-metastatic IIB-BR-G. Besides, other differentially overexpressed growth factors and/or their receptors in IIB-BR-G<sub>MTS6</sub> (i.e., EGFR, FGF2/bFGF, PDGF, PIGF, LAP-TGFβ1) could have led

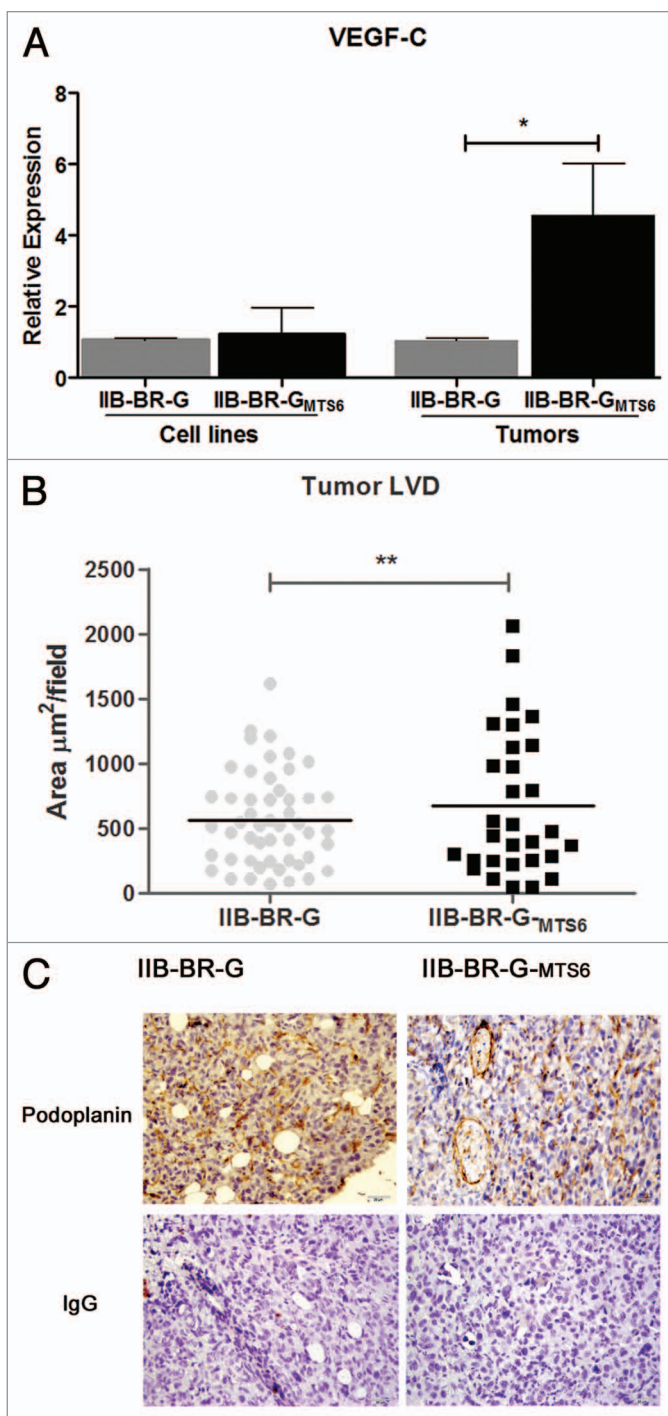


**Figure 3.** Lymphangiogenesis related analyses. (A) Relative VEGFC transcript abundances were measured by qPCR in tumor cell lines and xenografts as described under Materials and Methods. The expression fold changes were compared with the parental IIB-BR-G cell line or tumor, respectively. Results are mean ± SD of four biological replicates. \*Statistically significant  $p < 0.05$  (t-test). (B) LVD was calculated in Podoplanin stained sections of IIB-BR-G and IIB-BR-G<sub>MTS6</sub> xenografts as detailed under Materials and Methods. Dots represent each field count (Podoplanin-positive area/200× field), lines indicate the mean values. \*Statistically significant  $p < 0.05$  (t-test). (C) Examples of Podoplanin stainings in xenografted tumors and the corresponding negative controls (hamster IgG). Scale bar = 20 μm.

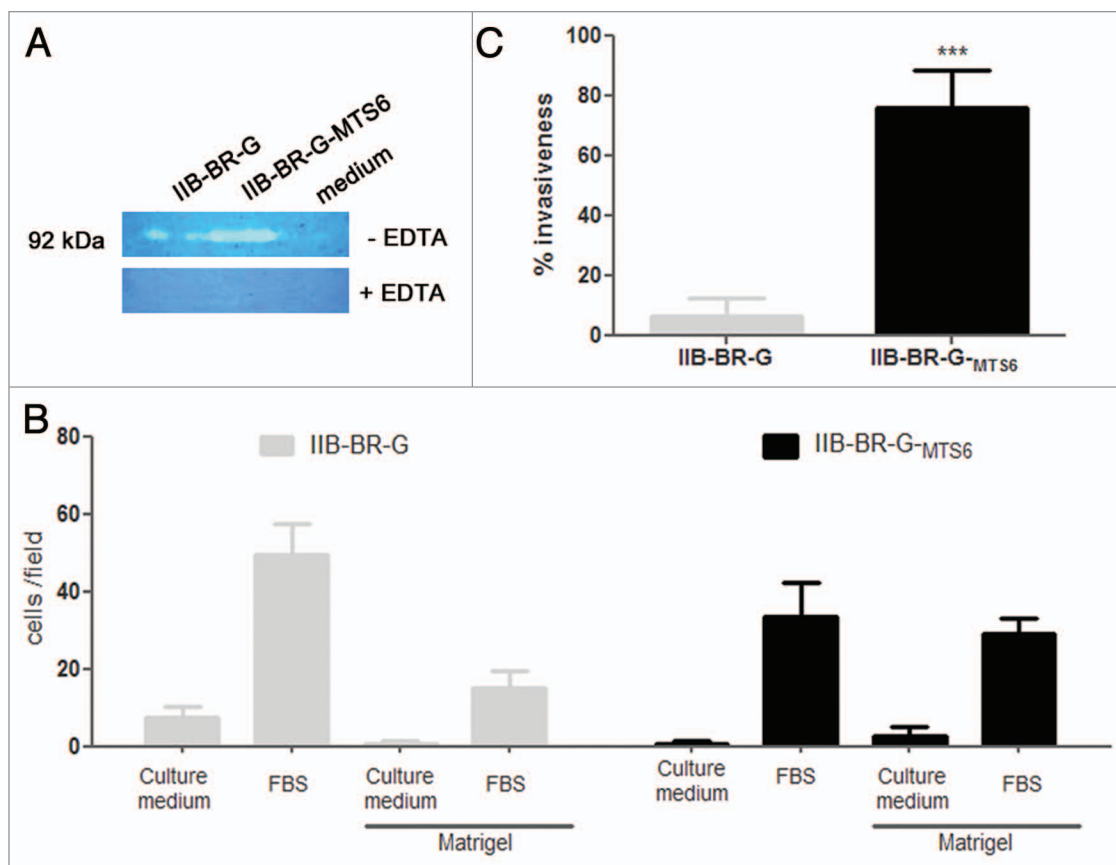


**Figure 4.** Invasiveness related in vitro analyses. (A) MMP9 zymography was performed in serum-free CM from both cell lines using gelatin as a substrate and Coomassie blue staining; the same samples were revealed in the presence of 20 mM EDTA to inhibit metalloprotease activity. A representative experiment is shown out of three independent determinations. (B) Number of cells that migrated through 8  $\mu$ m membrane and invaded matrigel were counted using culture medium plus 10% FBS as chemoattractant. (C) Relative invasiveness for each cell line was calculated. Results are shown as mean  $\pm$  SD.

to increased cell survival and proliferation, as evidenced by faster growth of IIB-BR-G-MTS6 vs IIB-BR-G xenografts in vivo.

IIB-BR-G-MTS6 upregulated IGFBPs 1, 3, 4 and 6. Deregulation of the IGF system is well recognized as a key contributor to the progression of multiple cancers including BC. Binding of IGFBP1 prolongs the half-life of the IGFs and alters their interaction with cell surface receptors. Interestingly, in pancreatic cancer, hypoxia has been shown to induce IGFBPs transcription contributing to reduce IGF signaling and to the survival of tumor cells.<sup>33</sup> Recent studies have demonstrated in MCF-7 breast cancer cells that IGF-I associates with vitronectin (VN) through IGFBP, and that IGF-I: IGFBP:VN complexes enhance cell migration and survival, processes central to metastasis.<sup>34</sup> During progression of BC extracellular matrix remodeling and a switch from estrogen dependence to EGFR dependence are accompanied by an increased expression of IGFBP3. IGFBP3 either inhibits or enhances EGF-mediated growth of breast epithelial cells, depending on the presence of fibronectin.<sup>35</sup> There is a number of reports suggesting that IGFBP3 can counterbalance IGFs effects. It has a negative effect on cell growth and survival.<sup>36</sup> This has led to the development of IGFBP3 as an anticancer therapeutic.<sup>37</sup> However, there are also many other reports that IGFBP3

can positively stimulate the proliferation<sup>38</sup> and survival<sup>39</sup> of various cells. In breast tumors the expression of IGFBP3 is positively associated with large, highly proliferative tumors and poor prognostic markers.<sup>40,41</sup> Thus, IGFBPs upregulation in IIB-BR-G-MTS6 cells could be associated to a lower IGF-signaling dependence for cell proliferation and survival and/or to the acquisition of a higher EGF-mediated metastatic growth in vivo.

FGF2/bFGF, upregulated in IIB-BR-G-MTS6 cells, has been very recently shown to promote the growth of TNBC in vitro and in vivo via an autocrine pathway that involves FGFR and thus points to a potential novel therapeutic approach using FGFR inhibitors for these tumors.<sup>42</sup>

IIB-BR-G-MTS6 s.c. tumors grow rapidly in nude mice and a central necrotic area is always observed by 5 weeks probably due to hypoxia (not shown). A hypoxic microenvironment often results in a milieu of pro-inflammatory and pro-angiogenic cytokines produced either by infiltrating cells and/or tumor cells. Since IIB-BR-G-MTS6 cells were selected in vivo, some of the proteins deregulated could reflect the interaction between fast growing tumor cells and an altered tumor stroma, as compared with IIB-BR-G slow growing tumors. Based on IIB-BR-G-MTS6 expression profile and recent publications,<sup>43</sup> we can speculate

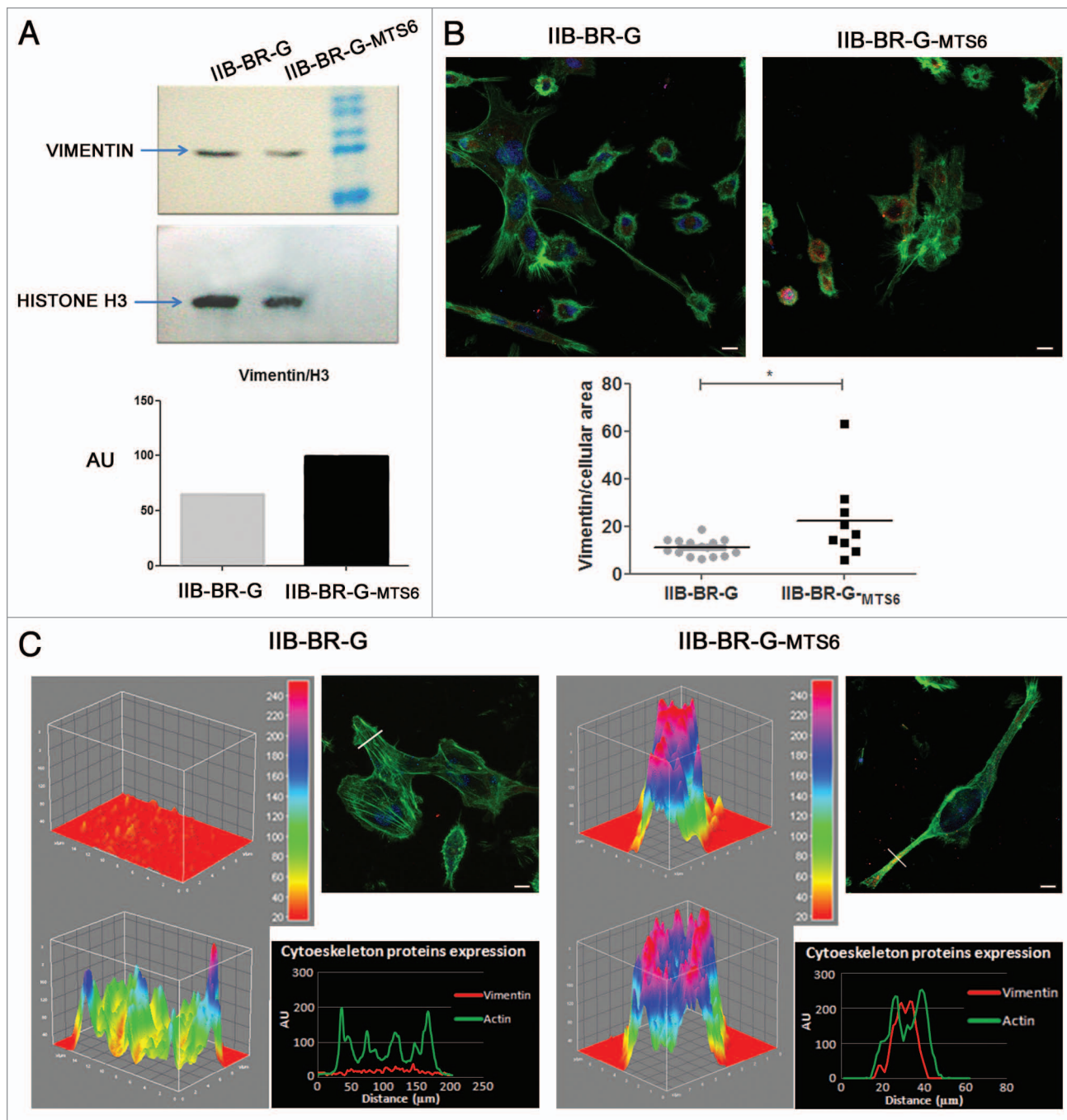


**Figure 5.** EMT in IIB-BR-G and IIB-BR-G<sub>MTS6</sub> cells. (A) Presence of mesenchymal marker vimentin. Western blot analysis was performed with cell extracts. A representative experiment is shown out of three independent determinations. Band intensities for vimentin were normalized to histone H3; AU = arbitrary units. (B) Confocal microscopy of IIB-BR-G and IIB-BR-G<sub>MTS6</sub> staining with anti-vimentin mAb (red) and actin microfilaments (green); scale bar = 10 μm. The relative intensities per area unit are shown below; \*statistically significant  $p < 0.05$  (t-test). (C) Spindle-shape morphology with cytoskeleton rearrangement determined by confocal microscopy as in (B) (top right), in IIB-BR-G and IIB-BR-G<sub>MTS6</sub>. The left panels are showing a computer-generated 3D surface plot profile image at the level of the segments delimited by the white line. And the bottom right plot profiles show distribution of actin and vimentin at a single plane of these segments. Scale bar = 5 μm.

that an elevated IL1 $\beta$ , IL6 production, and NF $\kappa$ B activation, as well as the production of pro-angiogenic factors might have been induced in response to hypoxia and high ROS (reactive oxygen species) generation in the tumor and/or stroma.

Throughout the metastatic selection process IIB-BR-G cells have acquired the expression of several pro-angiogenic and lymphangiogenic factors that probably contributed to tumor vascularization, accelerated tumor growth and conferred tumor cells the ability to colonize the lymphatic system to settle as a

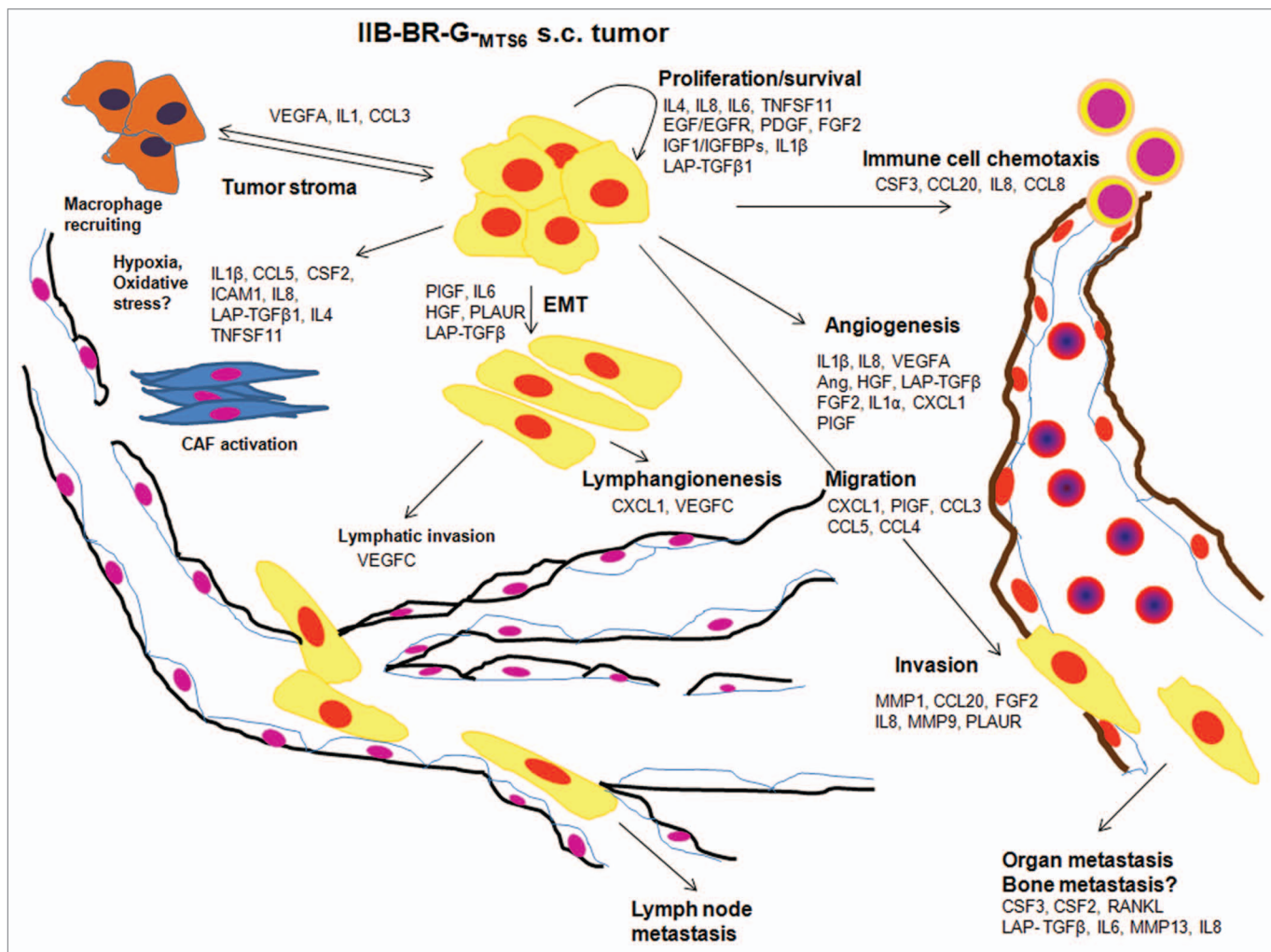


**Figure 6.** Proposed model for IIB-BR-G<sub>MTS6</sub> cells metastatic behavior suggested by their expression profile. Metastatic IIB-BR-G<sub>MTS6</sub> increased their proliferation rate in vivo probably by upregulation of growth factors and/or their receptors (i.e., EGFR, PDGF, IL1β), increased several pro-angiogenic factors (i.e., IL8, VEGF, HGF, FGF2 and IL1β), and enhanced their EMT phenotype by autocrine production of EMT inducers (i.e., IL6, PIGF, HGF, PLAUR and LAP-TGFβ). Cells could have acquired invasive capacity through MMPs secretion, and induced lymphangiogenesis by VEGFC secretion. Other up-regulated proteins could presumably have a role in alteration of the tumor stroma, driven by hypoxia due to accelerated tumor growth, and immune cells recruitment to the tumor microenvironment. Altogether, these features might have facilitated metastatic dissemination of IIB-BR-G<sub>MTS6</sub> cells mainly to the LNs.

LN metastasis. In this sense, upregulation of VEGFA, IL8, IL1, CXCL1, HGF, ANG and FGF2 altogether could have endowed IIB-BR-G<sub>MTS6</sub> cells with some of these pro-angiogenic properties. IIB-BR-G<sub>MTS6</sub> pro-angiogenic profile and VEGFA/B expression in s.c. nude mice xenografts suggest the existence of tumor cell vasculogenesis (vasculogenic mimicry), encircling solid tumor cells/nests, besides the existence of peripheral angiogenesis. Placenta growth factor (PIGF), a member of the VEGF family, is also upregulated in IIB-BR-G<sub>MTS6</sub> cells compared with IIB-BR-G. PIGF promotes metastasis, the mobilization and recruitment of hematopoietic precursors from bone marrow and enhances blood vessel maturation by acting on VEGFR1-expressing smooth muscle cells/pericytes.<sup>44</sup> In IIB-BR-G<sub>MTS6</sub>, higher CXCL1 and IL8 production could have directly increased blood and lymphatic endothelia proliferation, thus facilitating spread of tumor cells to LNs. Additionally, IL6 and IL4 production is commonly

associated to a pro-angiogenic phenotype,<sup>45</sup> and consistently we observed their upregulation in IIB-BR-G<sub>MTS6</sub>.

Lymphangiogenesis is an important step in tumor progression. Although the earliest feature of disseminated disease in BC is regional LN involvement, little is known about the mechanisms displayed by cancer cells to interact with lymphatic endothelial cells and enter the lymphatic system. VEGFC has been characterized as a lymphangiogenic growth factor signaling via VEGFR2 and VEGFR3. VEGFC has been detected on endothelial and tumor cells<sup>46,47</sup> and mediates tumor lymphangiogenesis and invasion of the neoplastic cells into lymphatic vessels. Similar to VEGFC, VEGFD is also a ligand of VEGFR2 and VEGFR3 but its role in lymph node metastasis in breast cancer is still controversial. VEGFA also acts as a lymphangiogenic factor, and tumor-derived VEGFA promotes expansion of the lymphatic network within draining sentinel LN, even before tumors

metastasize.<sup>47</sup> In metastatic IIB-BR-G<sub>-MTS6</sub> we found higher VEGFA *in vitro* while VEGFC expression was upregulated only *in vivo*, but lower VEGFD/FIGF, as compared with IIB-BR-G. Lymphatic invasion was evident in IIB-BR-G<sub>-MTS6</sub> s.c. xenograft lymph node vessels and afferent LN vessels, although LVD in IIB-BR-G<sub>-MTS6</sub> and IIB-BR-G s.c. tumors was not significantly different. Previously, high expression of VEGFA and C, but not of D, has been associated to higher LVD, higher MVD (microvessel density), the presence of LN metastasis, distant metastasis and a shorter OS in primary invasive breast tumors.<sup>17</sup>

The metastatic potential of chemokines is in part attributed to their ability to induce the expression of MMPs. It is believed that MMPs play a central role in the metastatic cascade and their increased expression reportedly is associated to the invasion and metastasis of various malignant tumors.<sup>28</sup> Our results further support their importance in the metastatic process in BC. Urokinase (uPA) and its receptor (PLAUR) overexpression are strongly correlated with poor prognosis in a variety of malignant tumors including BC.<sup>48</sup> PLAUR levels in breast tumors and tumor stroma are inversely correlated with ER status.<sup>49</sup> Also, under hypoxia, PLAUR has been shown to activate diverse cell signaling pathways that cooperatively induce EMT and may promote cancer metastasis.<sup>50,51</sup> Of note, PLAUR could also contribute to HGF cleavage to its active form, inducing cell invasiveness and enhancing tumorigenicity.<sup>52</sup> In IIB-BR-G<sub>-MTS6</sub> cells MMP9, MMP2 and MMP13 are deregulated and PLAUR and HGF are also upregulated in comparison to IIB-BR-G cells.

Stromal contribution to tumor growth is considered as an important source of cytokines, growth and pro-angiogenic factors that help tumors to progress and metastasize. Some of the proteins overexpressed in IIB-BR-G<sub>-MTS6</sub> have been described as expressed by stromal cells rather than by tumor cells, such as FGF2 production from CAF (cancer-associated fibroblasts), and extracellular MMPs.<sup>28,53</sup>

Metastatic IIB-BR-G<sub>-MTS6</sub> most upregulated cytokine is IL1 $\beta$  as compared with IIB-BR-G. Secreted IL1 $\beta$  is strongly pro-inflammatory, potentiates tumor angiogenesis and the production of a network of invasiveness-promoting molecules as well as tumor-mediated suppression. In fact, it was shown that IL1 is frequently expressed in metastasis from patients with several types of cancer. IL1 $\beta$  is found expressed in most ER negative invasive BC and high serum levels correlated with patient's recurrence.<sup>44,54</sup> Alterations in IL1 genomic structure, patterns of expression and processing may have crucial effects in the oncogenic process. In some tumors IL1 $\beta$  also acts as an autocrine growth factor and various proteins induced by exogenous IL1 $\beta$  like MMPs, VEGF, FGF2, IL8 and MCP1 both in tumor and stroma cells,<sup>55</sup> are also coordinately upregulated in IIB-BR-G<sub>-MTS6</sub> as compared with IIB-BR-G. IIB-BR-G<sub>-MTS6</sub> secretes more IL1 $\alpha$  to CM than IIB-BR-G cells. This fact is intriguing since IL1 $\alpha$  is rarely secreted by other cells than macrophages and its expression in tumor cells is intracellular or membrane associated.<sup>56</sup> However, in melanoma, tumor secreted IL1 $\alpha$  was shown to induce expression of pro-metastatic genes like IL6 and IL8 both in tumor and stromal cells.<sup>57</sup> Particularly in BC, IL1 $\beta$  is expressed in 90% of invasive carcinomas and in advanced tumors high IL1 $\beta$  content

correlated well with parameters associated to tumors aggressiveness (ER negativity, p53 mutation, absence of bcl-2 and expression of pro-inflammatory cytokines). Our findings in metastatic IIB-BR-G<sub>-MTS6</sub> cells further support that IL1 $\beta$  manipulation in TNBC tumors could be an attractive target for cancer therapy research.

In our TNBC metastatic model, CXCL12 production may prevent LN metastasis since it was found downregulated in IIB-BR-G<sub>-MTS6</sub> as compared with parental IIB-BR-G cells. CXCL12 is a highly pleiotropic chemokine that has been implicated in the progression and site-specific metastasis of various cancers, including BC. Indeed, CXCL12 silencing has been shown to induce metastasis of breast and colon cancer cells and administration of CXCL12 has been proposed as a potential therapy to inhibit metastatic dissemination.<sup>24,25</sup> IIB-BR-G<sub>-MTS6</sub> cells injected in nude mice occasionally established in the lungs as small tumor emboli (data not shown) and we have not yet analyzed their possible metastasis to bone. Several factors that could potentially contribute to bone metastasis are significantly upregulated in IIB-BR-G<sub>-MTS6</sub> cells and/ or secreted into their CM, such as the known osteoclast activators CSF3, CSF2, TNFSF11 (RANKL), LAP-TGF $\beta$ 1, IL6, MMP13 and IL8.<sup>58</sup> Thus, during LN metastasis progression BC cells might also acquire the ability to further disseminate and colonize other distant sites like bone.

CCL20/MIP-3 $\alpha$ , a chemokine involved in the attraction of immature dendritic cells (DC) and their precursors, is among the five most upregulated proteins secreted into IIB-BR-G<sub>-MTS6</sub> CM as compared with IIB-BR-G. Only few reports have suggested a possible relationship between CCL20/MIP-3 $\alpha$  and BC metastasis. It has been reported that adipocyte culture medium stimulates invasiveness of MDA-MB-231 cell via CCL20 production.<sup>59</sup> It could be possible that CCL20 production by IIB-BR-G<sub>-MTS6</sub> cells could confer increased invasiveness without the requirement of adipocytes in the tumor environment.

Most tumors secrete immunosuppressive cytokines such as TGF $\beta$ , IL10 and VEGF.<sup>60</sup> In both cell lines we found IL10, IL4, LAP-TGF $\beta$ 1, MMP9, and VEGF expression, suggesting that *in vivo* tumors generated by IIB-BR-G and specially IIB-BR-G<sub>-MTS6</sub> cells, could create an immunosuppressive microenvironment favoring tumor growth and metastatic dissemination.<sup>61</sup>

IL8 recruits immune system cells to the tumor stroma that could contribute to an increase in angiogenesis *in vivo* and tumor growth. There is a co-regulation of IL8, CXCL1, CXCL3, CXCL5 and CXCL6 since their coding genes are located in chromosome 4q21, in a cluster that has a coordinated expression pattern,<sup>62</sup> as we observed in IIB-BR-G<sub>-MTS6</sub> cells. Secreted IL8 and CXCL1 activate endothelial CXCR1/2 receptors in a paracrine manner to cause robust endothelial cell proliferation, tube formation, and migration.<sup>63</sup>

Epithelial cells can acquire mesenchymal characteristics including flattened morphology and expression of vimentin filaments, a process named epithelial-to-mesenchymal-transition. EMT also leads to the acquisition of an invasive phenotype enabling cell migration into a new microenvironment and their differentiation into distinct cell types, allowing tumor progression and metastasis.<sup>64</sup> Several soluble factors and receptors that

are potential inducers of EMT are expressed by these cells lines, and some are upregulated in IIB-BR-G<sub>-MTS6</sub> cells, such as LAP-TGF $\beta$ , IL6, FGF9, HGF, EGF, MMP1, MMP9 and MMP13, as well as PLAUR. In order to extent its cytoplasm and/or to form invadopodia, the cell needs the active motility of intermediate filaments, as it has been determined for neurons, being the intermediate filaments which determine protrusions caliber.<sup>65</sup> Thus, IIB-BR-G<sub>-MTS6</sub> cells expressing higher vimentin content could correlate with a more invadopodial phenotype than IIB-BR-G cells.

After global gene expression studies five molecular subtypes of BC have been identified (Luminal A, Luminal B, Her-2-enriched, basal-like and claudin-low), each of them presenting unique biologic features and different prognosis.<sup>2,66</sup> Most TNBC are of the basal like or claudin-low subtypes. Claudin-low BC are of poor prognosis, enriched in tumor initiating cells (CD44<sup>high</sup>/CD24<sup>low</sup>) but show low or absent expression of genes involved in cell-cell junction, including claudin 3, 4 and 7 and E-cadherin. Also, claudin-low tumors are highly enriched in immune-related genes like IL6 and CXCL2 but express low levels of proliferation related genes like Ki67. Basal-like breast tumors instead show high mitotic index (Ki67<sup>+</sup>), high EGFR expression and are often chemotherapy responsive.<sup>67</sup> Both subtypes show significant features of EMT.

Based on their proteomic profile, IIB-BR-G and the metastatic derived IIB-BR-G<sub>-MTS6</sub> cells could represent a model of aggressive TNBC which have undergone significant EMT, since they show: (1) a lack of expression of hormone receptors, (2) a high expression of vimentin, Fracktalkine/CX3CL1 and EGFR, (3) an expression of IL6, LAP-TGF $\beta$  and MMPs, (4) a high motility and invasive capacity, (5) lack of E-cadherin expression, and (6) in case of IIB-BR-G<sub>-MTS6</sub> cells, fast tumor growth, a high in vitro invasiveness and metastatic ability in nude mice. Also, we have previously shown that these cells do not express cytokeratins 5/6, a feature that is found in most basal-like BC type tumors.<sup>14</sup> However, lack of E-cadherin expression, high vimentin expression, pronounced EMT and expression of multiple immune related cytokines could also reflect the claudin-low phenotype. Since we have not addressed claudins expression in this study we cannot truly define whether these cell lines represent basal like or claudin-low TNBC.

In this study we report the development of a reproducible model to study the biology of human TNBC metastasis to LN in comparison with the parental non-metastatic cells. We succeeded in isolating a variant line with enhanced metastatic properties as demonstrated by a battery of assays.

We showed that IIB-BR-G<sub>-MTS6</sub> metastatic cells exhibited significant protein expression changes as compared with the parental non-metastatic cell line and have different phenotypic characteristics associated to their metastatic behavior, probably reflecting changes that occurred during progression from primary tumor growth and metastatic dissemination.

The up- and downregulation of proteins in IIB-BR-G<sub>-MTS6</sub> cells suggest interesting candidates for further investigation in TNBC metastasis. These cell lines offer an in vivo model which should facilitate in-depth studies to understand the features of

TNBC progression, the interaction of metastatic TNBC cells with host microenvironment and to test potential targets for biologically-based new therapies for TNBC.

## Materials and Methods

**IIB-BR-G<sub>-MTS6</sub> cells generation.** We generated IIB-BR-G<sub>-MTS6</sub> cell line after s.c. inoculation of  $1 \times 10^6$  cells of IIB-BR-G-MT2 cell line,<sup>14</sup> either in the mammary fat pad or in the back of 8 week old female mice N:NIH(S)-Fox1nu (Bioterio Universidad Nacional de La Plata, Argentina). After excision of LN metastasis, separation of tumor cells, amplification in few culture passages and s.c. re-inoculation in nude mice were performed. This procedure was repeated four times to enrich the tumor population with metastatic cells. In total, after six rounds of enrichment IIB-BR-G<sub>-MTS6</sub> cell line was obtained, amplified in culture to conform a stock and used for further experiments (Fig. 1A). Animals were maintained in a special facility in a ventilated Rack provided with HEPA filtered air in an Animal Facility at the Fundación Instituto Leloir-IIBBA (CONICET), in accordance with the guidelines of the NIH (Guide for the Care and Use of Laboratory Animals, 1996). The authors have received permission from the Institutional Animal Care and Use Committee for the nude mice experiments.

**Cell growth in vitro.** IIB-BR-G and IIB-BR-G<sub>-MTS6</sub> cell lines were grown as previously described.<sup>14</sup> Cell growth curves were performed in quadruplicate by the MTT assay as previously described.<sup>68</sup> Anchorage independent growth ability was estimated in triplicate by the soft agar clonogenic assay as previously described.  $5 \times 10^3$  tumor cells were seeded and colonies were counted under an Olympus CKX41 microscope (Olympus) after 21 d culture.

**Cell growth in vivo.** IIB-BR-G and IIB-BR-G<sub>-MTS6</sub> cells [ $1 \times 10^6/0.1$  ml phosphate buffered saline (PBS)] were injected s.c either in the mammary fat pad or the back of 8-week-old female nude mice. The tumors major and minor axes were measured with a caliper once a week. The tumor volumes were calculated using the formula:  $A^2 \times B/2$  where A = minor axis and B = major axis. Mice were euthanized with carbon monoxide; tumors were excised and samples were either formalin fixed or stored fresh at  $-80^\circ\text{C}$  with RNAlater (Ambion) for RNA and protein extraction.

**Antibody-based protein array.** The expression of 168 proteins was tested simultaneously with a glass chips based Human Cytokine Antibody Array System G (RayBio Series G-2000 Series, slides VI, VII and VIII, AAH-CYT-G2000-8, RayBiotech) following the manufacturer's protocol. Protein extracts and serum-free conditioned medium (CM) from either IIB-BR-G or IIB-BR-G<sub>-MTS6</sub> cell lines, were prepared following the manufacturer's protocol. Cell pellets were extracted with lysis buffer for 30 min and protein concentration was estimated by Bradford's method.<sup>69</sup> CM was collected after 24 h culture of exponentially growing cells in serum-free culture medium. Briefly, after blocking the glass chips were incubated with cell extracts (100  $\mu\text{g}$  total protein) or non-diluted CM (100  $\mu\text{l}$ ) overnight at  $4^\circ\text{C}$ . After washing steps chips were incubated with the corresponding biotin-conjugated antibodies for 2 h at room temperature (RT)

and then washed four times. Finally, slides were incubated with fluorescent dye-conjugated streptavidin for 2 h at RT in the dark and then washed. After complete drying the slides were scanned with an Axon Confocal Laser Scanner (GenePix 4000B, Axon Instruments) and images were processed with GenePix Pro 5.0 software.

**Data processing and analysis.** Data were normalized to positive controls of each slide with the RayBiotech Analysis Tool (RayBiotech) and relativization was performed after local background correction and subtraction for each of the three slides. Each protein was tested in duplicate and median signal values 2-fold above negative controls were considered positive. Fold change in expression was calculated as  $\log_2$  of signal IIB-BR-G<sub>-MTS6</sub>/signal IIB-BR-G. The threshold of significant difference in fold change for each protein was considered as  $\log_2$  signal IIB-BR-G<sub>-MTS6</sub>/signal IIB-BR-G > 1 or < -1, meaning that the protein is more than two times up or downregulated in IIB-BR-G<sub>-MTS6</sub> as compared with IIB-BR-G cells, respectively. Values between 1 and -1 were considered unchanged protein expression.

EASE software (DAVID, The Database for Annotation, Visualization and Integrated Discovery) was used to identify main gene categories differentially expressed by IIB-BR-G<sub>-MTS6</sub> cells in comparison with IIB-BR-G. Ease scores < 0.05 were considered significant. We also searched PubMed manually to investigate the biological relevance of genes that were up- and down-regulated.

**Immunostaining.** Formalin-fixed, paraffin-embedded sections were prepared with IIB-BR-G and IIB-BR-G<sub>-MTS6</sub> cell pellets and/or tumor sections (4  $\mu$ m) and stained using the following primary mAbs: mouse anti-human VEGF (A and B) (a kind gift from Dr Alberto Baldi, IByME, Buenos Aires, Argentina), mouse anti-human E-cadherin (clone NCH-38, Dako), mouse anti-human CD31 (clone JC70, Cell Marque) (both evaluated with an irrelevant mouse IgG (Sigma) as a negative control) and hamster anti-mouse Podoplanin/gp36 (Abcam) (Hamster IgG as negative control). Immunostaining pretreatments consisted of sample dehydration in graded alcohols, enzyme digestion, or other heat mediated retrieval methods. Sections were stained using either Envision labeled polymer-HRP K4003 (Dako) or ABC system (Vectastain Universal Elite ABC kit, PK-6200, Vector Laboratories) and counterstained with hematoxylin.

**Indirect immunofluorescence assays.** Cells grown on polylysine-coated coverslips were fixed with 4% paraformaldehyde and permeabilized with 0.1% triton X-100 in PBS. Fluorescence microscopy was performed in a LSM10 Meta confocal microscope (Carl Zeiss). Image analysis for immune localizations was performed using the 3D-surface plot plug-in of the Image-J program (v.1.42) from the NIH. Signal quantification and cytoplasmic redistribution were analyzed as previously described.<sup>70</sup> The reagents used were monoclonal IgM anti-vimentin (ascites) from Sigma Chemical Co., phalloidin-labeled microfilaments from Molecular Probes and Hoechst (Sigma).

**Western blotting.** Samples were lysed with 50 mM TRIS-HCl (pH 7.5), 5 mM EDTA, 150 mM NaCl, 1% NP-40, 0.1% SDS, in presence of Protease Inhibitor Cocktail (Sigma) for 30 min on ice. Protein extracts were obtained after centrifugation

at 8,000  $\times$  g for 10 min at 4°C and total protein concentration was measured by the Bradford assay. Thirty micrograms protein extracts were loaded onto 10% SDS-PAGE gels. Proteins were transferred onto nitrocellulose membranes (Sigma), blocked with 3% dried skim milk in PBS and then incubated with anti-vimentin mAbs (Clone VI-01, Abcam) and an anti-Histone H3 mAb (clone A3S, Upstate) (Sigma) overnight at 4°C. Binding of the mAbs was revealed using Alkaline Phosphatase (AP)-conjugated goat F(ab)<sub>2</sub> anti-mouse IgG(H+L) (Jackson ImmunoResearch). Color development substrate was 5-bromo-4-chloro-3-indolyl-phosphate/nitro blue tetrazolium (NBT/BCIP) (Promega).

**qPCR for VEGFC determination.** RT-PCR was performed with the isolated total RNA (1  $\mu$ g). RT-PCR was performed with using 5 ng random primers and the cDNA was synthesized using 200 units of MMLV-Reverse Transcriptase (Promega) at 37°C for 60 min. Real time PCR analysis was performed using specific primers designed to target unique regions of the cDNA. PCR runs were performed using SYBR Universal Master Mix (Applied Biosystems), and relative expression levels were determined by the  $\Delta\Delta$ Ct method using  $\beta$ -actin gene expression to normalize all samples. Both melting curve analysis and gel electrophoresis assessment were used to confirm the specificity of PCR reactions. The following cycling parameters were used: denaturation 95°C (1 min), annealing 56°C (1 min), extension and detection 72°C (30 sec). The cycler software was used for quantification of VEGFC mRNA levels relative to  $\beta$ -actin mRNA expression. Primers for VEGFC: forward 5'-CCT CAG CAA GAC GTT ATT TGA AAT T-3' and reverse 5'-TGG CAA AAC TGA TTG TTA CTG GTT-3'; for  $\beta$ -actin: forward 5'-CCA GAG GCG TAC AGG GAT AG-3' and reverse 5'-CCA ACC GCG AGA AGA TGA-3'.

**In vitro migration and invasion assay.** In vitro migration and invasion assays were performed using 8  $\mu$ m pore polycarbonate membrane transwells (BD Biosciences). For migration assay uncoated membranes were used while for invasion assay membranes were coated with 5  $\mu$ g/ml Matrigel (BD Biosciences). Cells were seeded in the upper chamber ( $5 \times 10^4$  cells/well) in serum-free culture medium and incubated at 37°C for 4h. Culture medium plus 10% fetal bovine serum (FBS, Natocor) was used as chemoattractant. Following incubation, the medium was discarded from the upper chamber and the entire insert plate was removed for staining procedures. Membranes were fixed with cold methanol, stained with Giemsa and mounted onto glass slides with Canadax. Cells were counted under the microscope. Five 200 $\times$  fields/condition and three wells/condition were analyzed. Results are expressed as in Equation 1:

$$\%invasion = \frac{\text{mean of cells invaded through Matrigel matrix coated membranes toward chemoattractant}}{\text{mean of cells invaded through uncoated membranestoward chemoattractant}} \times 100$$

**Zymography of matrix metalloproteinases using gelatin substrate.** Condition media were obtained incubating  $5 \times 10^5$  cells of each cell line in 1.5 ml DMEM for 24 h. The media were then collected and stored at -80°C until assayed. To analyze

the expression of metalloproteinases gelatin zymography was performed as previously described.<sup>71</sup> Briefly, 15  $\mu$ l conditioned medium (CM) from IIB-BR-G and IIB-BR-G<sub>-MTS6</sub> cells were fractionated in 10% native PAGE containing 0.1% gelatin as substrate. After electrophoresis, gels were incubated for 1 h at RT in Triton X-100 renaturing buffer and subsequently overnight at 37°C in developing buffer to allow enzymatic degradation of gelatin. The same assay was performed in the presence of 20 mM EDTA to inhibit the enzymatic reaction. After washing, the gels were stained with 0.125% Coomassie brilliant blue staining buffer and subsequently destained to visualize degradation bands. Molecular weight markers were used to determine the size of active enzymes. Pictures were documented with a trans-illuminator and a digital camera and the area of digestion was quantified using Image-J program (v.1.42) from the NIH software.

**Angiogenesis and lymphangiogenesis analysis in vivo.** Sections were examined by optical microscopy (Olympus BX40) and pictures were captured with 400 $\times$  magnification (Olympus Digital Camera DP72). To quantify VEGFA/B, CD31 and Podoplanin stainings at least 5 representative pictures from IIB-BR-G or IIB-BR-G<sub>-MTS6</sub> xenografts (n = 5) were analyzed using Fiji software. After setting the positive staining threshold, total positive areas were calculated for each picture.

To avoid duplications, the observation was made in a greek embroidery fashion. To separate immunostaining (brown stain) from hematoxylin staining (blue stain) the Color Threshold plug-in was applied. Images were then transformed into an 8-bit gray scale TIFF format. The number of stained structures was then counted. Data values obtained from at least 10 images of

each slide were exported to a spreadsheet in order to perform the statistical analysis.

**Statistics.** Comparisons between IIB-BR-G and IIB-BR-G<sub>-MTS6</sub> were analyzed using Student's t-test to determine the p values. p < 0.05 was considered significant.

#### Disclosure of Potential Conflicts of Interest

No potential conflicts of interest were disclosed.

#### Acknowledgments

This work has been supported by grants from the Agencia Nacional de Promoción Científica y Tecnológica (ANPCyT), Consejo Nacional de Investigaciones Científicas y Técnicas (CONICET), Fundación Sales, Fundación Cáncer (FUCA), Fundación Pedro F. Mosoteguy and Fundación María Calderón de la Barca, Argentina. M.B., E.L., J.M. and M.M.B. are members of CONICET, and M.P.R., J.M.A. and H.R.Q. are fellows of the same Institution. The authors are grateful to Dr Alberto Baldi for generous provision of anti-VEGFA/B antibody, Dr Jean-Luc Teillaud from Centre de Recherche des Cordeliers, Université Pierre et Marie Curie, Paris, France, for critically reading the manuscript, and to Vet. Adriana Fontanals from the Animal Care Facility, Fundación Instituto Leloir, IIBBA-CONICET, for her dedicated assistance. We thank the Pathology Department of Instituto Alexander Fleming and María Luisa Poljak for their support.

#### Supplemental Material

Supplemental materials may be found here:

<http://www.landesbioscience.com/journals/cbt/article/21187/>

#### References

- Sorlie T. Molecular portraits of breast cancer: tumour subtypes as distinct disease entities. *Eur J Cancer* 2004; 40:2667-75; PMID:15571950; <http://dx.doi.org/10.1016/j.ejca.2004.08.021>.
- Prat A, Parker JS, Karginova O, Fan C, Livasy C, Herschkowitz JL, et al. Phenotypic and molecular characterization of the claudin-low intrinsic subtype of breast cancer. *Breast Cancer Res* 2010; 12:R68; PMID:20813035; <http://dx.doi.org/10.1186/bcr2635>.
- Dent R, Trudeau M, Pritchard KI, Hanna WM, Kahn HK, Sawka CA, et al. Triple-negative breast cancer: clinical features and patterns of recurrence. *Clin Cancer Res* 2007; 13:4429-34; PMID:17671126; <http://dx.doi.org/10.1158/1078-0432.CCR-06-3045>.
- Gonzalez-Angulo AM, Timms KM, Liu S, Chen H, Litton JK, Potter J, et al. Incidence and outcome of BRCA mutations in unselected patients with triple receptor-negative breast cancer. *Clin Cancer Res* 2011; 17:1082-9; PMID:21233401; <http://dx.doi.org/10.1158/1078-0432.CCR-10-2560>.
- Thomas PA, Kirschmann DA, Cerhan JR, Folberg R, Sefter EA, Sellers TA, et al. Association between keratin and vimentin expression, malignant phenotype, and survival in postmenopausal breast cancer patients. *Clin Cancer Res* 1999; 5:2698-703; PMID:10537332.
- Laakso M, Tanner M, Nilsson J, Wiklund T, Erikstein B, Kellokumpu-Lehtinen P, et al. Basolateral carcinoma: a new biologically and prognostically distinct entity between basal and luminal breast cancer. *Clin Cancer Res* 2006; 12:4185-91; PMID:16857790; <http://dx.doi.org/10.1158/1078-0432.CCR-06-0353>.
- Dent R, Hanna WM, Trudeau M, Rawlinson E, Sun P, Narod SA. Pattern of metastatic spread in triple-negative breast cancer. *Breast Cancer Res Treat* 2009; 115:423-8; PMID:18543098; <http://dx.doi.org/10.1007/s10549-008-0086-2>.
- Hernandez-Aya LE, Chavez-Macgregor M, Lei X, Meric-Bernstam F, Buchholz TA, Hsu L, et al. Nodal status and clinical outcomes in a large cohort of patients with triple-negative breast cancer. *J Clin Oncol* 2011; 29:2628-34; PMID:21606433; <http://dx.doi.org/10.1200/JCO.2010.32.1877>.
- Aktas B, Müller V, Tewes M, Zeitz J, Kasimir-Bauer S, Loehberg CR, et al. Comparison of estrogen and progesterone receptor status of circulating tumor cells and the primary tumor in metastatic breast cancer patients. *Gynecol Oncol* 2011; 122:356-60; PMID:21605893; <http://dx.doi.org/10.1016/j.ygyno.2011.04.039>.
- Fabi A, Di Benedetto A, Metro G, Perracchio L, Nisticò C, Di Filippo F, et al. HER2 protein and gene variation between primary and metastatic breast cancer: significance and impact on patient care. *Clin Cancer Res* 2011; 17:2055-64; PMID:21307144; <http://dx.doi.org/10.1158/1078-0432.CCR-10-1920>.
- Guarneri V, Giovannelli S, Ficarra G, Bettelli S, Maiorana A, Piacentini F, et al. Comparison of HER-2 and hormone receptor expression in primary breast cancers and asynchronous paired metastases: impact on patient management. *Oncologist* 2008; 13:838-44; PMID:18650259; <http://dx.doi.org/10.1634/theoncologist.2008-0048>.
- Niikura N, Liu J, Hayashi N, Mittendorf EA, Gong Y, Palla SL, et al. Loss of human epidermal growth factor receptor 2 (HER2) expression in metastatic sites of HER2-overexpressing primary breast tumors. *J Clin Oncol* 2012; 30:593-9; PMID:22124109; <http://dx.doi.org/10.1200/JCO.2010.33.8889>.
- Bover L, Barrio M, Slavutsky I, Bravo AI, Quintans C, Bagnati A, et al. Description of a new human breast cancer cell line, IIB-BR-G, established from a primary undifferentiated tumor. *Breast Cancer Res Treat* 1991; 19:47-56; PMID:1661624; <http://dx.doi.org/10.1007/BF01975204>.
- Bover L, Barrio M, Bravo AI, Slavutsky I, Larriva I, Bolondi A, et al. The human breast cancer cell line IIB-BR-G has amplified c-myc and c-fos oncogenes in vitro and is spontaneously metastatic in vivo. *Cell Mol Biol (Noisy-le-grand)* 1998; 44:493-504; PMID:9620446.
- Roberti MP, Barrio MM, Bravo AI, Rocca YS, Arriaga JM, Bianchini M, et al. IL-15 and IL-2 increase Cetuximab-mediated cellular cytotoxicity against triple negative breast cancer cell lines expressing EGFR. *Breast Cancer Res Treat* 2011; 130:465-75; PMID:21308409; <http://dx.doi.org/10.1007/s10549-011-1360-2>.
- Todaro M, Lombardo Y, Francipane MG, Alea MP, Cammareri P, Iovino F, et al. Apoptosis resistance in epithelial tumors is mediated by tumor-cell-derived interleukin-4. *Cell Death Differ* 2008; 15:762-72; PMID:18202702; <http://dx.doi.org/10.1038/sj.cdd.4402305>.
- Mohammed RA, Green A, El-Shikh S, Paish EC, Ellis IO, Martin SG. Prognostic significance of vascular endothelial cell growth factors -A, -C and -D in breast cancer and their relationship with angiogenic and lymphangiogenesis. *Br J Cancer* 2007; 96:1092-100; PMID:17353919; <http://dx.doi.org/10.1038/sj.bjc.6603678>.
- Walton KL, Mankanji Y, Chen J, Wilce MC, Chan KL, Robertson DM, et al. Two distinct regions of latency-associated peptide coordinate stability of the latent transforming growth factor-beta1 complex. *J Biol Chem* 2010; 285:17029-37; PMID:20308061; <http://dx.doi.org/10.1074/jbc.M110.110288>.

19. Yu Q, Stamenkovic I. Cell surface-localized matrix metalloproteinase-9 proteolytically activates TGF-beta and promotes tumor invasion and angiogenesis. *Genes Dev* 2000; 14:163-76; PMID:10652271.
20. Hildenbrand R, Schaaf A. The urokinase-system in tumor tissue stroma of the breast and breast cancer cell invasion. *Int J Oncol* 2009; 34:15-23; PMID:19082473.
21. Singh S, Shi Q, Bailey ST, Palczewski MJ, Pardee AB, Iglehart JD, et al. Nuclear factor-kappaB activation: a molecular therapeutic target for estrogen receptor-negative and epidermal growth factor receptor family receptor-positive human breast cancer. *Mol Cancer Ther* 2007; 6:1973-82; PMID:17620428; <http://dx.doi.org/10.1158/1535-7163.MCT-07-0063>.
22. Biswas DK, Martin KJ, McAlister C, Cruz AP, Graner E, Dai SC, et al. Apoptosis caused by chemotherapeutic inhibition of nuclear factor-kappaB activation. *Cancer Res* 2003; 63:290-5; PMID:12543776.
23. Chavey C, Bibeau F, Gourgou-Bourgade S, Burlinon S, Boissière F, Laune D, et al. Oestrogen receptor negative breast cancers exhibit high cytokine content. *Breast Cancer Res* 2007; 9:R15; PMID:17261184; <http://dx.doi.org/10.1186/bcr1648>.
24. Apte RN, Dotan S, Elkabets M, White MR, Reich E, Carmi Y, et al. The involvement of IL-1 in tumorigenesis, tumor invasiveness, metastasis and tumor-host interactions. *Cancer Metastasis Rev* 2006; 25:387-408; PMID:17043764; <http://dx.doi.org/10.1007/s10555-006-9004-4>.
25. Drury LJ, Ziarek JJ, Gravel S, Veldkamp CT, Takekoshi T, Hwang ST, et al. Monomeric and dimeric CXCL12 inhibit metastasis through distinct CXCR4 interactions and signaling pathways. *Proc Natl Acad Sci U S A* 2011; 108:17655-60; PMID:21990345; <http://dx.doi.org/10.1073/pnas.1101133108>.
26. Taylor AR, Leon E, Goldenberg DM. Placental growth factor (PlGF) enhances breast cancer cell motility by mobilising ERK1/2 phosphorylation and cytoskeletal rearrangement. *Br J Cancer* 2010; 103:82-9; PMID:20551949; <http://dx.doi.org/10.1038/sj.bjc.6605746>.
27. Chan AY, Raft S, Bailly M, Wyckoff JB, Segall JE, Condeelis JS. EGF stimulates an increase in actin nucleation and filament number at the leading edge of the lamellipod in mammary adenocarcinoma cells. *J Cell Sci* 1998; 111:199-211; PMID:9405304.
28. Zlotnik A, Burkhardt AM, Homey B. Homeostatic chemokine receptors and organ-specific metastasis. *Nat Rev Immunol* 2011; 11:597-606; PMID:21866172; <http://dx.doi.org/10.1038/nri3049>.
29. Wilson J, Balkwill F. The role of cytokines in the epithelial cancer microenvironment. *Semin Cancer Biol* 2002; 12:113-20; PMID:12027583; <http://dx.doi.org/10.1006/scbi.2001.0419>.
30. Boon T, Van den Eynde B. Tumour immunology. *Curr Opin Immunol* 2003; 15:129-30; PMID:12633660; [http://dx.doi.org/10.1016/S0952-7915\(03\)00010-4](http://dx.doi.org/10.1016/S0952-7915(03)00010-4).
31. Vargo-Gogola T, Rosen JM. Modelling breast cancer: one size does not fit all. *Nat Rev Cancer* 2007; 7:659-72; PMID:17721431; <http://dx.doi.org/10.1038/nrc2193>.
32. O'Hayer KM, Brady DC, Counter CM. ELR+ CXC chemokines and oncogenic Ras-mediated tumorigenesis. *Carcinogenesis* 2009; 30:1841-7; PMID:19805574; <http://dx.doi.org/10.1093/carcin/bgp198>.
33. Koga T, Endo H, Miyamoto Y, Mukai M, Akira S, Inoue M. IGF1s contribute to survival of pancreatic cancer cells under severely hypoxic conditions. *Cancer Lett* 2008; 268:82-8; PMID:18467023; <http://dx.doi.org/10.1016/j.canlet.2008.03.030>.
34. Kashyap AS, Hollier BG, Manton KJ, Satyamoorthy K, Leavesley DI, Upton Z. Insulin-like growth factor-I-vitronectin complex-induced changes in gene expression effect breast cell survival and migration. *Endocrinology* 2011; 152:1388-401; PMID:21303956; <http://dx.doi.org/10.1210/en.2010-0897>.
35. McIntosh J, Dennison G, Holly JM, Jarrett C, Frankow A, Foulstone EJ, et al. IGF1R-3 can either inhibit or enhance EGF-mediated growth of breast epithelial cells dependent upon the presence of fibronectin. *J Biol Chem* 2010; 285:38788-800; PMID:20851879; <http://dx.doi.org/10.1074/jbc.M110.177311>.
36. Baxter RC. Signalling pathways involved in antiproliferative effects of IGF1R-3: a review. *Mol Pathol* 2001; 54:145-8; PMID:11376125; <http://dx.doi.org/10.1136/mp.54.3.145>.
37. Lee HY, Moon H, Chun KH, Chang YS, Hassan K, Ji L, et al. Effects of insulin-like growth factor binding protein-3 and farnesyltransferase inhibitor SCH66336 on Akt expression and apoptosis in non-small-cell lung cancer cells. *J Natl Cancer Inst* 2004; 96:1536-48; PMID:15494604; <http://dx.doi.org/10.1093/jnci/djh286>.
38. Kansra S, Ewton DZ, Wang J, Friedman E. IGF1R-3 mediates TGF beta 1 proliferative response in colon cancer cells. *Int J Cancer* 2000; 87:373-8; PMID:10897042; [http://dx.doi.org/10.1002/1097-0215\(20000801\)87:3<373::AID-IJC10>3.0.CO;2-X](http://dx.doi.org/10.1002/1097-0215(20000801)87:3<373::AID-IJC10>3.0.CO;2-X).
39. McCaig C, Fowler CA, Laurence NJ, Lai T, Savage PB, Holly JM, et al. Differential interactions between IGF1R-3 and transforming growth factor-beta (TGF-beta) in normal vs cancerous breast epithelial cells. *Br J Cancer* 2002; 86:1963-9; PMID:12085194; <http://dx.doi.org/10.1038/sj.bjc.6600355>.
40. Rocha RL, Hilsenbeck SG, Jackson JG, Lee AV, Figueroa JA, Yee D. Correlation of insulin-like growth factor-binding protein-3 messenger RNA with protein expression in primary breast cancer tissues: detection of higher levels in tumors with poor prognostic features. *J Natl Cancer Inst* 1996; 88:601-6; PMID:8609661; <http://dx.doi.org/10.1093/jnci/88.9.601>.
41. Vestey SB, Perks CM, Sen C, Calder CJ, Holly JM, Winters ZE. Immunohistochemical expression of insulin-like growth factor binding protein-3 in invasive breast cancers and ductal carcinoma in situ: implications for clinicopathology and patient outcome. *Breast Cancer Res* 2005; 7:R119-29; PMID:15642160; <http://dx.doi.org/10.1186/bcr963>.
42. Sharpe R, Pearson A, Herrera-Abreu MT, Johnson D, Mackay A, Welti JC, et al. FGFR signaling promotes the growth of triple-negative and basal-like breast cancer cell lines both in vitro and in vivo. *Clin Cancer Res* 2011; 17:5275-86; PMID:21712446; <http://dx.doi.org/10.1158/1078-0432.CCR-10-2727>.
43. Bulua AC, Simon A, Maddipati R, Pelletier M, Park H, Kim KY, et al. Mitochondrial reactive oxygen species promote production of proinflammatory cytokines and are elevated in TNFR1-associated periodic syndrome (TRAPS). *J Exp Med* 2011; 208:519-33; PMID:21282379; <http://dx.doi.org/10.1084/jem.20102049>.
44. Donnini S, Machein MR, Plate KH, Weich HA. Expression and localization of placenta growth factor and PlGF receptors in human meningiomas. *J Pathol* 1999; 189:66-71; PMID:10451490; [http://dx.doi.org/10.1002/\(SICI\)1096-9896\(199909\)189:1<66::AID-PATH390>3.0.CO;2-X](http://dx.doi.org/10.1002/(SICI)1096-9896(199909)189:1<66::AID-PATH390>3.0.CO;2-X).
45. Joyce JA, Pollard JW. Microenvironmental regulation of metastasis. *Nat Rev Cancer* 2009; 9:239-52; PMID:19279573; <http://dx.doi.org/10.1038/nrc2618>.
46. Kaplan RN, Riba RD, Zacharoulis S, Bramley AH, Vincent L, Costa C, et al. VEGFR1-positive haematopoietic bone marrow progenitors initiate the pre-metastatic niche. *Nature* 2005; 438:820-7; PMID:16341007; <http://dx.doi.org/10.1038/nature04186>.
47. Sloan EK, Priceman SJ, Cox BF, Yu S, Pimentel MA, Tangkanangkul V, et al. The sympathetic nervous system induces a metastatic switch in primary breast cancer. *Cancer Res* 2010; 70:7042-52; PMID:20823155; <http://dx.doi.org/10.1158/0008-5472.CAN-10-0522>.
48. Han B, Nakamura M, Mori I, Nakamura Y, Kakudo K. Urokinase-type plasminogen activator system and breast cancer (Review). [Review]. *Oncol Rep* 2005; 14:105-12; PMID:15944776.
49. Giannopoulou I, Mylona E, Kapranou A, Mavrommatis J, Markaki S, Zoumbouli Ch, et al. The prognostic value of the topographic distribution of uPAR expression in invasive breast carcinomas. *Cancer Lett* 2007; 246:262-7; PMID:17319000; <http://dx.doi.org/10.1016/j.canlet.2006.03.003>.
50. Lester RD, Jo M, Montel V, Takimoto S, Gonias SL. uPAR induces epithelial-mesenchymal transition in hypoxic breast cancer cells. *J Cell Biol* 2007; 178:425-36; PMID:17664334; <http://dx.doi.org/10.1083/jcb.200701092>.
51. Jo M, Takimoto S, Montel V, Gonias SL. The urokinase receptor promotes cancer metastasis independently of urokinase-type plasminogen activator in mice. *Am J Pathol* 2009; 175:190-200; PMID:19497996; <http://dx.doi.org/10.2353/ajpath.2009.081053>.
52. Bauer TW, Liu W, Fan F, Camp ER, Yang A, Somcio RJ, et al. Targeting of urokinase plasminogen activator receptor in human pancreatic carcinoma cells inhibits c-Met- and insulin-like growth factor-I receptor-mediated migration and invasion and orthotopic tumor growth in mice. *Cancer Res* 2005; 65:7775-81; PMID:16140945.
53. Giulianelli S, Cerliani JP, Lamb CA, Fabris VT, Bottino MC, Gorostiaga MA, et al. Carcinoma-associated fibroblasts activate progesterone receptors and induce hormone independent mammary tumor growth: A role for the FGF-2/FGFR-2 axis. *Int J Cancer* 2008; 123:2518-31; PMID:18767044; <http://dx.doi.org/10.1002/ijc.23820>.
54. Singer CF, Hudelist G, Gschwanter-Kaulich D, Fink-Retter A, Mueller R, Walter I, et al. Interleukin-1alpha protein secretion in breast cancer is associated with poor differentiation and estrogen receptor alpha negativity. *Int J Gynecol Cancer* 2006; 16(Suppl 2):556-9; PMID:17010072; <http://dx.doi.org/10.1111/j.1525-1438.2006.00695.x>.
55. Lewis AM, Varghese S, Xu H, Alexander HR. Interleukin-1 and cancer progression: the emerging role of interleukin-1 receptor antagonist as a novel therapeutic agent in cancer treatment. *J Transl Med* 2006; 4:48; PMID:17096856; <http://dx.doi.org/10.1186/1479-5876-4-48>.
56. Apte RN, Voronov E. Interleukin-1--a major pleiotropic cytokine in tumor-host interactions. *Semin Cancer Biol* 2002; 12:277-90; PMID:12147202; [http://dx.doi.org/10.1016/S1044-579X\(02\)00014-7](http://dx.doi.org/10.1016/S1044-579X(02)00014-7).
57. Nozaki S, Sledge GW Jr, Nakshatri H. Cancer cell-derived interleukin 1alpha contributes to autocrine and paracrine induction of pro-metastatic genes in breast cancer. *Biochem Biophys Res Commun* 2000; 275:60-2; PMID:10944441; <http://dx.doi.org/10.1006/bbrc.2000.3241>.
58. Weilbaecher KN, Guise TA, McCauley LK. Cancer to bone: a fatal attraction. *Nat Rev Cancer* 2011; 11:411-25; PMID:21593787; <http://dx.doi.org/10.1038/nrc3055>.
59. Kim KY, Baek A, Park YS, Park MY, Kim JH, Lim JS, et al. Adipocyte culture medium stimulates invasiveness of MDA-MB-231 cell via CCL20 production. *Oncol Rep* 2009; 22:1497-504; PMID:19885605.
60. Gabrilovich DI, Chen HL, Girgis KR, Cunningham HT, Meny GM, Nadaf S, et al. Production of vascular endothelial growth factor by human tumors inhibits the functional maturation of dendritic cells. *Nat Med* 1996; 2:1096-103; PMID:8837607; <http://dx.doi.org/10.1038/nm1096-1096>.
61. Gocheva V, Wang HW, Gadea BB, Shree T, Hunter KE, Garfall AL, et al. IL-4 induces cathepsin protease activity in tumor-associated macrophages to promote cancer growth and invasion. *Genes Dev* 2010; 24:241-55; PMID:20080943; <http://dx.doi.org/10.1101/gad.1874010>.

62. Bièche I, Chavey C, Andrieu C, Busson M, Vacher S, Le Corre L, et al. CXC chemokines located in the 4q21 region are up-regulated in breast cancer. *Endocr Relat Cancer* 2007; 14:1039-52; PMID:18045955; <http://dx.doi.org/10.1677/erc.1.01301>.
63. Agarwal A, Tressel SL, Kaimal R, Balla M, Lam FH, Covic L, et al. Identification of a metalloprotease-chemokine signaling system in the ovarian cancer microenvironment: implications for antiangiogenic therapy. *Cancer Res* 2010; 70:5880-90; PMID:20570895; <http://dx.doi.org/10.1158/0008-5472.CAN-09-4341>.
64. Thomson S, Petti F, Sujka-Kwok I, Mercado P, Bean J, Monaghan M, et al. A systems view of epithelial-mesenchymal transition signaling states. *Clin Exp Metastasis* 2011; 28:137-55; PMID:21194007; <http://dx.doi.org/10.1007/s10585-010-9367-3>.
65. Cleveland DW, Monteiro MJ, Wong PC, Gill SR, Gearhart JD, Hoffman PN. Involvement of neurofilaments in the radial growth of axons. *J Cell Sci Suppl* 1991; 15:85-95; PMID:1824110.
66. Prat A, Perou CM. Deconstructing the molecular portraits of breast cancer. *Mol Oncol* 2011; 5:5-23; PMID:21147047; <http://dx.doi.org/10.1016/j.molonc.2010.11.003>.
67. Badve S, Dabbs DJ, Schnitt SJ, Bachner FL, Decker T, Eusebi V, et al. Basal-like and triple-negative breast cancers: a critical review with an emphasis on the implications for pathologists and oncologists. *Mod Pathol* 2011; 24:157-67; PMID:21076464; <http://dx.doi.org/10.1038/modpathol.2010.200>.
68. Freimoser FM, Jakob CA, Aebi M, Tuor U. The MTT [3-(4,5-dimethylthiazol-2-yl)-2,5-diphenyltetrazolium bromide] assay is a fast and reliable method for colorimetric determination of fungal cell densities. *Appl Environ Microbiol* 1999; 65:3727-9; PMID:10427074.
69. Bradford MM. A rapid and sensitive method for the quantitation of microgram quantities of protein utilizing the principle of protein-dye binding. *Anal Biochem* 1976; 72:248-54; PMID:942051; [http://dx.doi.org/10.1016/0003-2697\(76\)90527-3](http://dx.doi.org/10.1016/0003-2697(76)90527-3).
70. Quintá HR, Maschi D, Gomez-Sanchez C, Pwien-Pilipuk G, Galigniana MD. Subcellular rearrangement of hsp90-binding immunophilins accompanies neuronal differentiation and neurite outgrowth. *J Neurochem* 2010; 115:716-34; PMID:20796173; <http://dx.doi.org/10.1111/j.1471-4159.2010.06970.x>.
71. Simian M, Molinolo A, Lanari C. Involvement of matrix metalloproteinase activity in hormone-induced mammary tumor regression. *Am J Pathol* 2006; 168:270-9; PMID:16400029; <http://dx.doi.org/10.2353/ajpath.2006.050012>.